Overexpression of FOXO1 enhances CAR T cell polyfunctionality, metabolic fitness and efficacy against solid tumors

Paul Beavis

Paul.Beavis@petermac.org

Peter MacCallum Cancer Centre https://orcid.org/0000-0002-2116-013X

Phillip Darcy

Peter MacCallum Cancer Centre https://orcid.org/0000-0002-5303-9561

Junyun Lai

Peter MacCallum Cancer Centre https://orcid.org/0000-0001-5884-2786

Jack Chan

Peter MacCallum Cancer Centre https://orcid.org/0000-0002-5942-8592

Kevin Sek

Peter MacCallum Cancer Centre https://orcid.org/0000-0003-4634-7600

Christina Scheffler

Peter MacCallum Cancer Centre https://orcid.org/0000-0003-3731-6204

Isabelle Munoz

Peter MacCallum Cancer Centre https://orcid.org/0000-0001-6510-5696

Yu-Kuan Huang

Peter MacCallum Cancer Centre https://orcid.org/0000-0003-2262-7069

Kah Min Yap

Peter MacCallum Cancer Centre

Joel Lee

Peter MacCallum Cancer Centre

Jasmine Li

Peter MacCallum Cancer Centre

Amanda Chen

Peter MacCallum Cancer Centre

Cheok Weng Chan

Peter MacCallum Cancer Centre

Emily Derrick

Peter MacCallum Cancer Centre https://orcid.org/0000-0001-7191-3948

Kirsten Todd

Peter MacCallum Cancer Centre https://orcid.org/0000-0002-3903-166X
Junming Tong
Peter MacCallum Cancer Centre
Maria N. de Menezes
Peter MacCallum Cancer Centre
Emma Petley
WEHI
Joelle Kim
Peter MacCallum Cancer Centre
Dat Nguyen
Peter MacCallum Cancer Centre
Patrick Leung
Peter MacCallum Cancer Centre
Joan So
Peter MacCallum Cancer Centre https://orcid.org/0000-0001-6550-0637
Christian Deo Deguit
Peter MacCallum Cancer Centre https://orcid.org/0000-0003-0759-4035
Joe Zhu
Peter MacCallum Cancer Centre https://orcid.org/0000-0003-4416-7040
Imran House
Peter MacCallum Cancer Centre https://orcid.org/0000-0002-6245-5954
Lev Kats
Peter MacCallum Cancer Centre https://orcid.org/0000-0001-8742-8138
Jane Oliaro
Peter MacCallum Cancer Centre https://orcid.org/0000-0002-2097-6428
Ian Parish
Peter MacCallum Cancer Centre https://orcid.org/0000-0003-3528-478X
Kylie Quinn
Peter MacCallum Cancer Centre https://orcid.org/0000-0002-0417-3625
Paul Neeson
Peter MacCallum Cancer Centre https://orcid.org/0000-0002-2729-5887
Clare Slaney
Peter MacCallum Cancer Centre
Nicole Saw
Peter MacCallum Cancer Centre
Phoebe Dunbar
Peter MacCallum Cancer Centre
Jiawen Li
Peter MacCallum Cancer Centre

Thang Hoang
Peter MacCallum Cancer Centre
Benjamin Solomon
Peter MacCallum Cancer Centre https://orcid.org/0000-0003-3059-5730
Simon Harrison
Peter MacCallum Cancer Centre https://orcid.org/0000-0003-4555-6582
Andrew Scott
Olivia Newton John Cancer Research Institute

Biological Sciences - Article

Keywords: CAR T cells, solid tumor, polyfunctionality, exhaustion, differentiation, Foxo1, Tcf7, Id3

Posted Date: November 3rd, 2023

DOI: https://doi.org/10.21203/rs.3.rs-2584153/v1

Additional Declarations: There is **NO** Competing Interest.

Version of Record: A version of this preprint was published at Nature on April 10th, 2024. See the published version at https://doi.org/10.1038/s41586-024-07242-1.

Overexpression of FOXO1 enhances CAR T cell polyfunctionality, metabolic fitness and efficacy against solid tumors.

Jack D. Chan[1,2*], Christina Scheffler[1,2*], Isabelle Munoz[1,2*], Kevin Sek[1,2], Joel Lee[1,2], Yu-Kuan Huang[1,2], Kah Min Yap[1,2], Nicole Y.L. Saw[1,2], Jasmine Li[1,2], Amanda X.Y. Chen[1,2], Cheok Weng Chan[1,2], Emily B. Derrick[1,2], Kirsten L. Todd[1,2], Junming Tong[1,2], Phoebe A. Dunbar[1,2], Jiawen Li[1,2], Thang X. Hoang[1,2], Maria N. de Menezes[1,2] Emma V. Petley[1,2], Joelle S. Kim[1,2], Dat Nguyen[1,2], Patrick S.K. Leung[3], Joan So[2], Christian Deguit[1,2], Joe Zhu[1,2], Imran G. House[1,2], Lev M Kats[2], Andrew M. Scott[5,6], Benjamin J. Solomon[2], Simon J. Harrison[2,7], Jane Oliaro[1,2], Ian A. Parish[1,2], Kylie M. Quinn[3,4], Paul J. Neeson[1,2], Clare Y. Slaney[1,2], Junyun Lai[1,2+], Paul A. Beavis[1,2+], Phillip K. Darcy[1,2,7+]

[1]Cancer Immunology Program, Peter MacCallum Cancer Centre, Melbourne, 3000, Victoria, Australia.
[2]Sir Peter MacCallum Department of Oncology, The University of Melbourne, Parkville, 3010, Australia.
[3]School of Health and Biomedical Sciences, RMIT University, Bundoora, 3083, VIC
[4] Department of Biochemistry and Molecular Biology, Monash University, Clayton, 3800, VIC
[5]Olivia Newton-John Cancer Research Institute, and School of Cancer Medicine, La Trobe University, Melbourne, VIC 3086, Australia.
[6]Faculty of Medicine, The University of Melbourne, Parkville, 3010, Australia.
[7]Clinical Haematology and Centre of Excellence for Cellular Immunotherapies, Peter MacCallum Cancer Centre and Royal Melbourne Hospital, Melbourne, Vic, Australia.
[8] Department of Immunology, Monash University, Clayton.

[*] Contributed equally
[+] Senior authors contributed equally

Address correspondence and reprint requests to Paul A. Beavis (paul.beavis@petermac.org) Junyun Lai (junyun.lai@petermac.org) or Phillip K. Darcy (phil.darcy@petermac.org), Cancer Immunology Program, Peter MacCallum Cancer Centre, Victoria, Australia.

Key words: CAR T cells, solid tumor, polyfunctionality, exhaustion, differentiation, Foxo1, Tcf7, Id3

This work was funded by a National Breast Cancer Foundation Grant (IIRS-22-095), a Program Grant and an Ideas grant from the National Health and Medical Research Council (NHMRC; Grant number 1132373 and 2012475). J.D. Chan was supported by an Australian Government Research Training Program scholarship and a Peter MacCallum Cancer Foundation post graduate scholarship. J. Lai was supported by a Cancer Research Institute Irvington Postdoctoral Fellowship (#CRI 3530). P. A. Beavis was supported by a National Breast Cancer Foundation Fellowship (ID# ECF-17-005, 2017-2020) and a Victorian Cancer Agency Mid-Career Fellowship (2021-Current). I.G. House was supported by a Victorian Cancer Agency Early Career Fellowship (ECRF20017). A.M. Scott was supported by an NHMRC Investigator Fellowship (No. 1177837) P. K. Darcy was supported by an NHMRC Senior Research Fellowship (APP1136680). The authors wish to acknowledge the contribution of consumer representatives Karen Gill, Mike Rear and Graeme Sissing for their contribution to the study and research direction of the laboratory.

Abstract

The efficacy of chimeric antigen receptor (CAR) T cell therapy is limited in solid tumors by several factors including the immunosuppressive tumor microenvironment that gives rise to poorly persisting and metabolically dysfunctional T cells. To overcome this, we sought to identify transcription factors that could enhance CAR T cell fitness. We identified that the overexpression of Foxo1 could enhance the therapeutic efficacy of murine CAR T cells in the setting of syngeneic immunocompetent models and was dependent on the sustained production of proinflammatory cytokines. FOXO1 overexpression in human CAR T cells enforced broad transcriptional and epigenetic changes that led to a more “stem-like” phenotype and similarly improved therapeutic efficacy. Enhanced efficacy was associated with improved mitochondrial fitness and persistence in vivo. FOXO1 overexpression also led to a more stem like phenotype in patient derived CAR T cells and is therefore a promising strategy for the treatment of solid cancers.

Introduction

Chimeric antigen receptor (CAR) T cell therapy using autologous gene-modified T cells expressing a single chain variable fragment (scFv) recognizing a tumor-associated antigen has shown remarkable effects in certain B cell hematological cancers (1-3). However, CAR T cell therapy has largely been ineffective in the treatment of solid tumors. This is due to several reasons, including poor CAR T cell persistence and polyfunctionality (4, 5). In the solid tumor microenvironment (TME), adoptively transferred CAR T cells are pre-disposed to terminally differentiate due to chronic antigen stimulation, metabolic competition in the TME and lack of appropriate co-stimulatory signals (6, 7). Terminally differentiated CAR T cells are similar to exhausted endogenous T cells that fail to eliminate tumors due to dysfunction, attenuated effector function and poor persistence (6, 7). Such cells are characterized by the production of low levels of effector molecules such as inflammatory cytokines, the expression of immune checkpoint co-inhibitory receptors including PD-1, LAG3 and TIM3, and are phenotypically characterized by expression of transcriptional regulators including TOX and IRF4 (6-9).

Recently, it has been demonstrated that less differentiated CAR T cells are more effective at immune-mediated control of tumors relative to more terminally differentiated effector T cells (7, 10). This is due to less differentiated T cells maintaining higher multipotency and a greater self-renewal capacity. These cells have increased long-term persistence and can generate terminally differentiated effector cell progeny to facilitate improved tumor control (11, 12). Accordingly, patient products that contain initial higher frequencies of less differentiated CAR T cells have improved persistence and therapeutic potential (13, 14).

The process of T cell differentiation and epigenetic reprogramming are heavily dependent on each other. In terms of CAR T cells, the immunosuppressive environment of the solid tumor microenvironment drives CAR T cells towards an exhausted phenotype characterized by sub-optimal functions that are enforced by epigenetic regulations such as repressive DNA methylation at key gene loci. (15, 16). Increasing evidence suggests that the metabolic profile of CAR T cells is critical for their persistence and polyfunctionality, with improved oxidative metabolism and increased mitochondrial biogenesis being associated with enhanced CAR T cell persistence and function (17-19). A number of pre-clinical studies have explored a variety of methods and approaches to favorably modulate CAR T cell differentiation before adoptive transfer. These include the use or expression of homeostatic cytokines, co-stimulation,

epigenetic regulation and more recently, the overexpression of transcriptional regulators (6, 10, 20-22). For example, overexpression of c-Jun or BATF has been shown to restrict CAR T cell exhaustion, improve persistence and enhance therapeutic outcomes in solid tumor models (6, 20, 23). However, none of these genetic reprogramming approaches have identified a transcriptional regulator candidate that can rewire CAR T cells to enhance their metabolic fitness and protect them from exhaustion.

Our previous work has shown that preconditioning CAR T cells with IL-15 as opposed to IL-2 can enhance their persistence and polyfunctionality (24). Given that IL-15 has been shown to favorably modulate the metabolism of CAR T cells, but is only a transient effect observed while the cells are in culture, we sought to identify key transcription factors upregulated by IL-15 that are responsible for this effect (25). Analysis of the epigenome and transcriptome of IL-2 and IL-15 cultured CAR T cells revealed a strong enrichment of a *Foxo1* gene signature. Knockout of *Foxo1* led to a significant reduction of $CD62L^{+}TCF1^{+}$ CAR T cells, confirming the importance of this transcription factor in the maintenance of a less differentiated CAR T cell product. Conversely, overexpression of a constitutively active variant of Foxo1 (Foxo1-ADA) in murine anti-Her2 CAR T cells improved the production of inflammatory cytokines and metabolic fitness, ultimately leading to enhanced tumor control in adoptive transfer solid tumor models. Therapeutic effects exhibited by Foxo1-ADA overexpressing CAR T cells were shown to be dependent on increased cytokine production and Foxo1-ADA overexpression maintained CAR T cell polyfunctionality to a greater extent than other transcriptional regulators upregulated by IL-15, namely *Tcf7* and *Id3*. Similar results were achieved using human anti-Lewis Y CAR T cells engineered to overexpress FOXO1, where similar enhancement of metabolic fitness was observed leading to increased tumor infiltration and anti-tumor efficacy. FOXO1 overexpression implemented a transcriptional and epigenetic program that significantly enhanced CAR T cell stemness but importantly did not preclude FOXO1-expressing CAR T cells from acquiring robust effector function upon antigen stimulation. Overall, our findings show that overexpression of FOXO1 enhances CAR T cell efficacy in the treatment of solid tumors and provides promising groundwork to utilize this approach in a clinical setting.

Materials and Methods

Animal models

C57BL/6 wildtype (WT) mice and C57BL/6 human-Her2 (hHer2) transgenic mice were bred in the Peter MacCallum Cancer Centre animal facility. NOD.Cg-Prkdc scid IL2rg (NSG) mice were either bred at the Peter MacCallum Cancer Centre or obtained from Australian BioResources (Moss Vale, New South Wales). Mice used in experiments were between 6 to 16 weeks of age and were housed in PC2 specific pathogen-free conditions. Experiments were approved by the Animal Experimentation Ethics Committee #E582, #E671 and #E693.

Cell lines

The mouse MC38 colon adenocarcinoma cell line was provided by Dr Jeffrey Schlom (NIH, Bethesda, Maryland, USA). The mouse breast carcinoma cell line E0771 was obtained from Professor Robin Anderson (Olivia Newton-John Cancer Centre, Heidelberg, Victoria, Australia). The parental MC38 and E0771 tumor cell lines were retrovirally transduced with a murine stem cell virus (MSCV) vector to express a truncated hHer2 antigen that lacks intracellular signaling components. Transduced tumor cell lines are referred to as MC38-Her2 and E0771-Her2. OVCAR-3 and MCF7 tumor cells were obtained from the American Type Culture Collection. PCR analysis was used to verify that tumor lines were mycoplasma-negative.

Retroviral vector packaging cell lines PA317 and GP+e86 were obtained from American Type Culture Collection (ATCC). The GP+e86 and tumor cell lines were maintained in Roswell Park Memorial Institute (RPMI) media (Gibco Life Technologies) supplemented with 10% heat-inactivated fetal bovine serum (FBS), 1 mM sodium pyruvate, 2 mM glutamine, 0.1 mM non-essential amino acids, 10 mM 4-(2-hydroxyethyl)-1-piperazineethanesulfonic acid (HEPES), 100 U/mL penicillin and 100 μg/mL streptomycin. These cells were maintained at 37ºC in a humidified incubator with 5% CO_2. The PA317 cell line was maintained in Dulbecco's Modified Eagle's Medium (DMEM, Gibco) supplemented with 2 mM glutamine and 100 U/mL penicillin and 100 μg/mL streptomycin and was maintained in a humidified incubator at 37ºC with 10% CO_2.

Reagents and cytokines

Mouse α-IFNγ antibody (H22, IgG, catalogue number: BE0312) and the isotype control (2A3 clone, IgG2a, catalogue number: BE0254) antibody were purchased from BioXcell. The cytokine, IL-2 was obtained from the National Institutes of Health (NIH, Maryland, USA) and purchased from Peprotech. IL-7 and IL-15 were purchased from Peprotech. Where indicated CAR T cells were stimulated with an anti-idiotype antibody that was custom made.

Generation of retroviral packaging lines for the transduction of primary murine T cells

cDNA of murine Tcf7, Foxo1 (wild-type), Foxo1-ADA, Id3 and c-Jun were cloned into the murine stem cell virus (MSCV) vector encoding either an mCherry marker gene or truncated (lacks cell signaling components) human nerve growth factor receptor (NGFR). The viral packaging GP+e86 cell line that produces the anti-Her2 CAR retrovirus was generated as previously described (26, 27). The anti-Her2 CAR construct was comprised of an extracellular scFv specific for human Her2, an extracellular CD8 hinge region, a CD28 transmembrane domain and an intracellular CD3ζ domain. GP+e86 cell lines encoding both the anti-Her2 CAR and a transcriptional regulator were generated and the resulting anti-Her2 CAR packaging cells were sorted based on NGFR or mCherry expression by flow cytometry. Supernatants from these cells were used to transduce primary mouse T cells as previously described (28) and following transduction, CAR T cells were maintained in supplemented RPMI media with IL-7 (200 pg/mL), IL-15 (10 ng/mL) and β-mercaptoethanol (50 μM).

Generation of lentivirus for the transduction of human T cells

Lentiviral packaging plasmids (pCMV-VSV-G, pMDLg/pRRE, pRSV-Rev) and plasmid vectors encoding a second-generation anti-Lewis Y CAR and either FOXO1 WT, FOXO1-ADA or mCherry were purchased from GenScript. Briefly, packaging plasmids and transgene plasmids were transfected into HEK293T cells. Across the following 3 days, cell culture supernatants were harvested, pooled and centrifuged with Lenti-X-Concentrator (Takara Bio) to concentrate lentivirus. Lentivirus was used to transduce human T cells activated with OKT3 (30 ng/mL) and IL-2 (600 IU/mL) by adding virus directly to cell cultures at a MOI of 0.5 in Lentiboost (Sirion).

CRISPR/Cas9 editing of CAR T cells

CRISPR/Cas9 editing of murine CAR T cells was performed as previously described (24). Per 100 x 10^6 naïve splenocytes or 5 x 10^6 activated human PBMCs, 270 pmoles sgRNA (Synthego) and 37 pmoles recombinant Cas9 were combined and incubated for 10 minutes to generate Cas9/sgRNA RNP. Cells were resuspended in 20 µl P3 buffer (Lonza), combined with RNP and electroporated with a 4D-Nucleofector (Lonza) with pulse code E0115 or DN100 for human and mouse T cells, respectively. Prewarmed media was then added to cells for 10 minutes prior to activation and transduction of murine T cells or immediate transduction of human T cells. sgRNA sequences used were as follows: *Foxo1* Guide 1: 5' CACCUGGGGCGCUUCGGCCA 3' Guide 2: 5' CCACUCGUAGAUCUGCGACA 3'. *FOXO1* Guide 1 CACCUGAGGCGCCUCGGCCA

***In vitro* re-stimulation assay**

Tumor cell targets were co-cultured with CAR T cells at a 1:1 ratio for 24 hours. After overnight incubation, supernatants were harvested and an equivalent number of tumor cells were reseeded into the incubations for another 24 hours. This process was repeated one final time before cells were harvested for analysis by flow cytometry and supernatants were analyzed by cytometric bead array (CBA) utilizing either murine or human cytokine Flex sets (BD Biosciences) according to the manufacturer's instructions.

Flow cytometry and cell sorting

For flow cytometric analysis Fc receptor block (2.4G2 diluted 1:50 from hybridoma supernatant in FACS buffer) was added to cells for 10 minutes at 4°C. Cells were stained with 50 µL fluorochrome-conjugated antibody cocktails and incubated for 30 minutes in the dark at 4°C. For intracellular staining, cells were fixed and permeabilized using the eBioscience™ FoxP3 / Transcription Factor Staining Buffer Set (Thermofisher) according to the manufacturer's instructions. Samples were quantified using counting beads (Beckman Coulter; 20 µL per sample) using the following formula: number of beads per sample/bead events * cell events of interest. Cells were analyzed on a BD LSRFortessa or BD FACSymphony (BD Biosciences) and data was analyzed using Flowjo (TreesStar) or OMIQ (https://www.omiq.ai/). Cells were sorted using a BD FACSAria Fusion. To stain for intracellular Id3, formalin fixation and methanol permeabilization was utilized. Following extracellular staining, cells were fixed in 100 µL of 10% formalin for 10 minutes at room temperature. Cells were then washed twice in PBS and permeabilized in 100 µL of chilled 90%

methanol for 10 minutes on ice. Cells were washed once in PBS and stained with 50 µL of fluorochrome conjugated antibody cocktails made up in FACS buffer for 30 minutes in the dark at room temperature. Refer to the Supplementary Table for the list of antibodies used for flow cytometry.

Treatment of mice with CAR T cells

C57BL/6 human-Her2 transgenic mice were injected with 2 x 10^5 E0771-Her2 breast carcinoma cells orthotopically into the mammary fat pad 5-7 days prior to treatment or subcutaneously with 2.5 x 10^5 MC38-Her2 colon adenocarcinoma cells 5 days prior to treatment. After tumors were established, mice bearing E0771-Her2 or MC38-Her2 tumors were preconditioned with 4 Gy or 0.5 Gy total body irradiation respectively. Mice were then treated with intravenous doses of 1 x 10^7 CAR T cells on 2 consecutive days and one dose of IL-2 (50,000 IU/dose) with the first dose of CAR T cells, followed by two doses of IL-2 each day on the next 2 consecutive days. Tumor area was measured every 2-3 days following treatment. For IFNγ blockade experiments, mice were dosed with 250 µg of anti-IFNγ or isotype control antibody, 2A3, on days 0, 1 and 7 following CAR T cell treatment.

For experiments utilizing human anti-Lewis Y CAR T cells, NSG mice were injected with 5 x 10^6 OVCAR-3 tumor cells. Once tumors were established, at day 10-15 post injection, mice were treated with 1 Gy total body irradiation and intravenously treated with 2-5 x10^6 $Flag^+$ CAR T cells. Mice were treated with IL-2 as per experiments in the C57BL/6 human-Her2 transgenic model.

Analysis of immune subsets in tumor, spleen, draining lymph nodes and blood

Blood was collected via submandibular or retroorbital bleed into tubes containing EDTA prior to euthanasia. Blood and spleen samples were treated twice or once respectively with ACK lysis buffer before staining for flow cytometry. Tumors were digested in SAFC DMEM media (Gibco) with 0.01 mg/mL DNase (Sigma Aldrich) and 1 mg/mL type IV collagenase (Sigma Aldrich) for 30 minutes at 37ºC. Following digestion, tumor samples were filtered twice through a 70 µm filter to create a single cell suspension and resuspended in Fc block prior to staining for analysis by flow cytometry. For stimulation of intratumoral CAR T cells to assess cytokine secretion capacity, tumor cell suspensions were resuspended in complete RPMI media with 10 ng/mL phorbol 12-myristate 13-Acetate (PMA, Abcam), 1 µg/mL ionomycin (Abcam),

GolgiStop (1:1500 dilution, BD Biosciences) and GolgiPlug (1:1000 dilution, BD Biosciences). Samples were incubated for 3 hours at 37ºC with 5% CO_2 prior to staining for analysis by flow cytometry. Single cell suspensions from dLN were created by placing tissue between 2 pieces of 70 μm filter mesh in 400 μL of FACS buffer and by mechanically digesting using the end of a syringe. The resultant cell suspension was then stained for analysis by flow cytometry. For mitochondrial analysis, isolated cells were stained using Mitotracker Deep Red FM and Mitotracker Green FM (Thermofisher) according to the manufacturer's protocols.

Seahorse assay

A Seahorse XFe24 Bioanalyser (Agilent) was used to determine OCR for indicated CAR T cells prepared from 5 separate donors. Cells were washed in assay media (XF Base media (Agilent) with glucose (10 mM), sodium pyruvate (1 mM) and L-glutamine (2 mM) (Gibco), pH 7.4 at 37 °C) before being plated onto Seahorse cell culture plates coated with Cell-Tak (Corning) at $4x10^5$ cells per well. After adherence and equilibration, cellular oxygen consumption rates (OCR) and extracellular acidification rates (ECAR) were measured using a Seahorse MitoStress assay (Agilent), with addition of oligomycin (1 μM), carbonyl cyanide 4-(trifluoromethoxy) phenylhydrazone (FCCP; 1.2 μM) and antimycin A and rotenone (0.5 μM each). Assay parameters were as follows: 3 min mix, no wait, 3 min measurement, repeated 3 times at basal and after each addition. Raw OCR values were normalized to the amount of protein per well, as assessed by a Pierce BCA protein assay (ThermoFisher) performed as per manufacturer instructions. SRC was calculated as OCR at maximum rate − OCR in basal state.

Gene expression analysis

Following manufacturer's instructions, RNA-seq libraries were prepared from RNA using the Quant-seq 3′ mRNA-seq Library Prep Kit for Illumina (Lexogen). Single-end, 75bp RNA-sequencing was performed via NextSeq (Illumina, Inc., San Diego, CA) and CASAVA 1.8.2 was subsequently used for base calling. Cutadapt v2.1 was used to remove random primer bias and trim 3' end poly-A-tail derived reads. Quality control was assessed using FastQC v0.11.6 and RNA-SeQC v1.1.8 (29). Sequence alignment against the mouse reference genome mm10 or the human genome hg19 was performed using HISAT2. Finally, featureCounts from the Rsubread software package 2.10.5 was used to quantify the raw reads with genes defined from the respective Ensembl releases (30). Gene counts were normalized using the TMM (trimmed means of M-values) method and converted into log2 counts per million (CPM) using the EdgeR

package (31, 32). The quasi-likelihood F test statistical test method based on the generalized linear model (glm) framework from EdgeR was used for differential gene expression comparisons Adjusted p values were computed using the Benjamini-Hochberg method. Principal component analysis (PCA) was performed generated based on the top most variable genes. Differentially expressed genes (DEGs) were classified as significant based on a false discovery rate (FDR) cutoff of less than 0.05. For heatmaps, the pheatmap R package was used to plot row mean centered and scaled normalized log2(CPM+0.5) values. Genes columns or rows were sorted by hierarchical clustering using Euclidean distance and average-linkage.

Unbiased gene set enrichment analysis was performed using fgsea package on differential expressed genes pre-ranked by fold change with 1000 permutations (nominal P-value cutoff <0.05) (33). Reference gene sets were obtained from the MsigDB library for Hallmarks, KEGG (https://www.genome.jp/kegg/kegg1.html), CHEA dataset (34-37), or based upon previously published analyses of glycolysis signature (25), single-cell RNA sequencing derived T cell clusters in patients (38).

scRNA-seq data processing and analysis

CAR T cells were co-cultured with MCF7 tumor cells at a 1:1 ratio for 24 h. Fc-receptors were blocked with human FcBlock (BD BioSciences) for 10 min at 4 C before staining with 50 µL fluorochrome-conjugated antibody cocktail for 30 minutes in the dark at 4°C. Samples were labelled with anchor LMO (5'-TGGAATTCTCGGGTGCCAAGGgtaacgatccagctgtcact-[Lipid]-3), co-anchor LMO (5'-[Lipid]-AGTGACAGCTGGATCGTTAC-3') and sample specific barcodes for 5 min in the dark at 4°C. CAR^+ T cells were sorted by FACS and samples were pooled at equal ratios followed by staining with 100 ul TotalSeq-C anti-human CD4 and CD8 (BioLegend) antibody cocktail for 30 minutes in the dark at 4°C. scRNA-seq data were generated using the 10x Cell Ranger pipeline (7.1.0) and hg38 genome. Specifically, cellranger multi was used to generate raw feature barcode matrices. Downstream analysis was performed in R (version 4.2.0). Empty droplets were detected and removed from the raw feature barcode matrix using the emptyDrops function from the DropletUtils (version 1.16.0) package and doublets were detected and removed using DoubletFinder (verison 2.0.3). Using Seurat (version 4.3.0), cells with less than 200 features and more than 5% mitochondrial reads were excluded. Standard Seurat data processing and normalization steps were performed:

NormalizeData, FindVariableFeatures, ScaleData, RunPCA, RunUMAP, FindNeighbors and FindClusters; clusters with low-quality metrics were removed, and the final resolution was determined using results from the clustree package (version 0.5.0). Lipid-modified oligos (LMOs) were demultiplexed using HTODemux (Seurat). DEGs were calculated using the functions FindAllMarkers (Seurat) using a log2 fold-change threshold of 0.125 and an adjusted P value of less than 0.05, and included the number of counts as a latent variable. Pseudobulk DEGs were detected using the Libra package (version 1.0.0) using the run_de function. Gene-set enrichment was performed using the fgsea package with all expressed genes as the background gene list, which was ranked by average log fold-change detected with FindMarkers using a log2 fold-change threshold of 0 and min.pct parameter set to 0. To perform diffexp analyses and GSEA between individual groups within each cluster, the to_psuedobulk function from Libra was used to pull out pseudobulk count matrix of each replicate pool and clusters. EdgeR and fgsea was then utilized to perform differential expression and gsea analyses of reference gene signatures. The Single-cell signature explorer program was utilized for visualization of gene signatures across UMAP plots (39).

ATAC-Seq data analysis

Sequencing files for ATAC-seq experiments were demultiplexed using Bcl2fastq (v2.20) to generate Fastq files. Next QC of files were performed using FASTQC (v0.11.5). Adaptor trimming of paired-end reads was performed with NGmerge (v0.3) where required (40). Alignment of reads to either the reference human (hg38) or mouse (mm10) genome was performed using Bowtie2 (v2.3.3). The resulting SAM files were converted to BAM files using Samtools (v1.4.1) using the view command, which were subsequently sorted and indexed, with potential PCR duplicates marked with Samtools markdup. Peak calling was performed with either MACS2 (v2.1.1) or Genrich (v0.6.0) packages. Annotation of ATAC-Seq peaks to proximal genes was performed using either annotatePeaks.pl (Homer, v4.11) or the annotatePeak function from ChIPseeker R package (v1.8.6). BAM files were converted into BigWig files using the bamCoverage function (Deeptools, v3.5.0). BigWig files were then imported into Integrative Genomics Viewer (IGV, v2.7.0) for visualization of specific loci. To generate IgV style track plots from BigWig files, the package trackplot was used (41). The HOMER makeTagDirectory command was used to generate tag directories, and the findPeaks command was used to identify peaks, with the control tag directory set to respective control groups. Motif discovery using the findMotifsGenome tool and default settings identified de

novo motifs from peaks identified. The ChromVAR R package (42) was used to identify enriched motifs from the JASPAR 2022 database (43), in unstimulated or stimulated groups.

Statistical analysis

Statistical analyses were performed using GraphPad Prism. Analyses performed include paired or unpaired Student's t test to compare two data sets, one-way ANOVA to analyze multiple data sets across a single time point and two-way ANOVA when analyzing multiple sets of data across time.

Data availability

The RNA-Sequencing and ATAC-Sequencing data that supports the findings of this study have been deposited in GEO NCBI under the accession code GSE225527 that contains the subseries GSE225521, GSE225522, GSE225523 and GSE225526. Source data are available within the paper, supplementary information or available upon request from the authors.

Results

CAR T cells generated with IL-15 have increased expression of memory-associated transcriptional regulators

Previous studies by both our group and others have shown that CAR T cells generated with IL-7 and IL-15 display a less differentiated T cell phenotype and elicit greater long-term persistence relative to CAR T cells cultured in IL-2 and IL-7, which is linked to their reduced expression of glycolytic enzymes and improved mitochondrial fitness (24, 25, 44, 45). Indeed, CAR T cells cultured with IL-15 exhibited a more pronounced T_{CM} phenotype, characterized by an increased expression of CD62L and improved persistence in the spleen and tumors of E0771-Her2 tumor bearing mice (**Fig. 1a-b**). To interrogate the transcriptional regulation of this phenotype, we compared the epigenome and transcriptome of IL-15 and IL-2 generated $CD8^+$ CAR T cells that were sorted at day 7 post transduction. RNA-seq analysis revealed increased expression of genes associated with memory or persistence in IL-15 generated CAR T cells including *c-Jun*, *Tcf7* (which encodes for Tcf1), *Id3*, *Foxo1* and *Klf2*, a known Foxo1 target gene (2, 6, 46-49) (**Fig. 1c-d**). Furthermore, IL-15 induced a downregulation of glycolytic genes consistent with the notion that IL-15 induces a favorable metabolic phenotype (**Fig. 1e**)(25). Notably, analysis of the impact of IL-15 preconditioning on the transcriptional profile of CAR T cells revealed that Foxo1 target genes were the most significantly enriched subset based upon both a publicly available ChIP-seq dataset and a list of genes with at least one canonical FOXO1 binding motif within 2kb +/- of the transcriptional start site (**Fig. 1f-g**). At the epigenetic level, Foxo1 was also one of the highest ranking transcription factors. ATAC-seq analysis revealed a significant enrichment for Foxo1 binding motifs in genomic regions that became more accessible after culture in IL-15 as determined by both Homer (**Fig. 1h-i**) and ChromeVAR analyses (**Fig. 1j**). Interestingly, motif enrichment was also observed for Fli1, which has previously been shown to negatively regulate T cell persistence through antagonism of ETS:RUNX activity, Tcf7, a factor known to regulate memory formation and Tcf3, a transcription factor that is known to interact with Id3 (38, 50-52). Given the increased expression of Foxo1 target genes in IL-15 cultured CAR T cells, we interrogated the importance of Foxo1 in CAR T cell function through CRISPR/Cas9 mediated targeting. Consistent with a role in maintaining CAR T cells in a favorable differentiation state, deletion of Foxo1 in murine CAR T cells led to a significant reduction in CD62L expression and upon serial coculture with E0771-Her2 tumor cells led to a significant reduction in the proportion of

TCF1$^+$ cells and increased expression of TIM3, PD-1 and LAG3, altogether indicative of a transition to a more short-term effector like phenotype (**Fig 1k-m**).

Foxo1 overexpression enhances CAR T cell survival and polyfunctionality *in vitro*

Given the strong molecular signature of Foxo1 in IL-15 conditioned CAR T cells and the critical importance of Foxo1 in maintaining CAR T cell stemness, we next investigated the phenotype and function of Foxo1 overexpressing CAR T cells. Given T cell activation facilitates the exclusion of wild-type Foxo1 from the nucleus via post-translational modifications, we elected to overexpress a constitutively active variant of Foxo1, Foxo1-ADA, in murine anti-Her2 CAR T cells (53-55). Foxo1-ADA overexpressing CAR T cells were compared to CAR T cells expressing Tcf7, Id3 and c-Jun given previous data indicating the enhanced efficacy of c-Jun overexpressing CAR T cells (6, 23).

These transcriptional regulators were cloned into a retroviral plasmid that included the human NGFR reporter gene, where successfully transduced T cells expressed a truncated NGFR as a marker of transcriptional regulator overexpression. To assess the impact of selected transcriptional regulators, CAR T cells directed against human Her2 were generated, in line with our previous work, and their activity against Her2 expressing tumor cell lines evaluated. (24, 28). Successful transduction of T cells was confirmed via Myc-tagged CAR expression and overexpression of respective factors via qRT-PCR of sorted CD8$^+$NGFR$^+$ CAR T cells (**Supplementary Fig. 1a-b**). The effects of transcription factor overexpression were assessed *in vitro* via a re-stimulation assay, which involved re-stimulating CAR T cells with E0771-Her2 tumors three times before phenotypic and functional analysis of CAR T cells and cell culture supernatants (**Fig. 2a**).

Conventional CAR T cells lose their capacity to secrete interferon γ (IFNγ) and tumor necrosis factor (TNF) over multiple rounds of antigenic stimulation due to exhaustion or dysfunction. This limits their efficacy given that these cytokines are required for CAR T cell anti-tumor function (6, 20, 56-58). Remarkably, the overexpression of Tcf7 and Foxo1-ADA led to significantly increased IFNγ and TNF production relative to control CAR T cells after each successive round of stimulation (**Fig. 2b-c**). Moreover, Foxo1-ADA, and to a lesser extent c-Jun or Tcf7 overexpression led to significantly increased Granzyme B (GzmB) expression, suggestive of prolonged killing capacity (**Fig. 2d-e**). Importantly, the overexpression of either Foxo1-ADA, Tcf7, Id3 or c-Jun led to a significant increase in CAR T cell numbers and

maintenance of a less differentiated CAR T cell surface phenotype as indicated by the total number of $CD8^+$ CAR T cells including those exhibiting a $CD62L^+Ly108^+$ 'stem-like' phenotype (**Fig. 2f**).

Foxo1 overexpressing CAR T cells have enhanced *in vivo* anti-tumor efficacy, polyfunctionality and mitochondrial fitness

Having established that overexpression of pro-memory transcription factors enhanced CAR T cell polyfunctionality *in vitro*, we next investigated their *in vivo* anti-tumor potential in orthotopic breast tumor and colon carcinoma models. In this study we utilized an immunocompetent, transgenic C57BL/6-Her2 mouse model that expresses human Her2 in breast epithelial and brain tissue (59, 60). This mouse model permits the growth of Her2 expressing tumors and assessment of anti-Her2 CAR T cells in conditions that mimic the immunosuppressive tumor microenvironment encountered in clinical settings. In mice bearing orthotopic E0771-Her2 breast tumors or subcutaneous MC38-Her2 tumors, the overexpression of Tcf7, Foxo1-ADA or Id3 enhanced CAR T cell efficacy and led to more durable anti-tumor control and a significant increase in survival for mice treated with Foxo1-ADA or Id3-expressing CAR T cells relative to controls (**Fig. 2g-i**, **Supplementary Fig. 2a-c**). In a head-to-head comparison, whilst Foxo1-ADA expression enhanced CAR T cell function, the overexpression of c-Jun did not lead to a statistically significant enhancement of efficacy relative to control CAR T cells (**Supplementary Fig. 2d**). Notably, the overexpression of wild type Foxo1 did not significantly enhance therapeutic efficacy, indicating that the constitutively active form was necessary to improve the function of murine CAR T cells (**Supplementary Fig. 2e**).

We next investigated the *in vivo* phenotype of CAR T cells engineered to express the respective transcription factors. CAR T cells were isolated from tumors and draining lymph nodes of tumor bearing mice 9 days post treatment. Remarkably, CAR T cells overexpressing Foxo1-ADA exhibited significantly increased production of the pro-inflammatory cytokines IFNγ and TNF relative to control CAR T cells (**Fig. 3a**). CAR T cell polyfunctionality was assessed through quantification of the frequencies of cells expressing IFNγ, TNF and GzmB. Foxo1-ADA most significantly improved polyfunctionality as indicated by a higher frequency of CAR T cells expressing 2 or more effector molecules (IFNγ, TNF or GzmB) and was the only factor that harbored significantly fewer cells expressing none of the analyzed effector molecules

relative to control CAR T cells (**Fig. 3b**). Assessment of other parameters of $CD8^+$ CAR T cell function revealed that Foxo1-ADA overexpression led to only a modest increase in Ki67 expression both within the total $CD8^+$ CAR T cell population, and the $Tcf1^+$ less-differentiated subset (**Supplementary Fig. 3a-b)**. Similarly, Foxo1-ADA expressing CAR T cells also expressed comparable levels of the activation markers PD-1 and TIM3 relative to control CAR T cells, consistent with the notion that Foxo1-ADA expression did not prevent CAR T cells from acquiring an effector-like phenotype upon tumor antigen recognition (**Supplementary Fig. 3c**). Given the expression of PD-1 on these CAR T cells, we investigated whether therapeutic benefit could be augmented through the addition of immune checkpoint blockade therapy. Indeed, combination of Foxo1-ADA expressing CAR T cells with anti-PD-1 resulted in significantly improved tumor growth inhibition compared to control CAR T cells, suggesting synergy between Foxo1-ADA CAR T cells and PD-1 blockade **(Supplementary Fig. 3d)**. Next, we assessed the impact of transcription factor expression on the number and phenotype of $CD4^+$ CAR T cells. Consistent with our previous observations (24), $CD4^+$ CAR T cells made up only a minor proportion of tumor-infiltrating CAR T cells and this was not significantly modulated by expression of Tcf7, Id3 or Foxo1-ADA (**Supplementary Fig. 3e**).

Previously our group and others have shown that secretion of IFNγ is critical for CAR T cell anti-tumor efficacy in the solid tumor setting (58, 61, 62). Given that Foxo1-ADA expression led to enhanced cytokine production, the contribution of IFNγ to the therapeutic activity of Foxo1-ADA overexpressing CAR T cells was assessed. MC38-Her2 tumor bearing mice were treated with CAR T cells alone or in the context of IFNγ neutralization. These experiments revealed that IFNγ blockade abrogated the enhanced therapeutic activity of Foxo1-ADA overexpressing CAR T cells, indicating that IFNγ produced by Foxo1-ADA-expressing cells likely led to the enhanced therapeutic effects, confirming the important role of IFNγ in the effective treatment of solid tumors by CAR T cells (**Fig. 3c**).

To interrogate the relationship between overexpression of these transcription factors and metabolic function, we first investigated the impact of transcription factor expression on mitochondrial mass and fitness within intratumoral $CD8^+$ CAR T cells (47, 63). CAR T cells isolated from the tumors of treated mice were stained *ex vivo* with the mitochondrial dyes, Mitotracker Deep Red (MDR) and Mitotracker Green (MG) that are indicative of a properly regulated mitochondrial membrane potential and mitochondrial mass respectively. Strikingly,

compared to control CAR T cells, intratumoral CAR T cells overexpressing Tcf7 or Foxo1-ADA, but not Id3, displayed an increased ratio of cells with functional mitochondria (designated as MDR^{hi}/MG^{int-hi}, blue gate) relative to dysfunctional mitochondria ($MDR^{int}MG^{high}$; orange gate). This was also reflected by higher MDR and MG staining intensities, indicative of properly regulated membrane potential and mitochondrial mass (**Fig. 3d-e**) (64). Enhanced mitochondrial fitness of Foxo1-ADA expressing CAR T cells was co-rroborated through RNA-sequencing of *in vitro* stimulated Foxo1-ADA overexpressing CAR T cells. This analysis revealed that an oxidative phosphorylation signature was amongst the most significantly upregulated pathways in Foxo1-ADA expressing CAR T cells relative to control CAR T cells (**Fig. 3f, Supplementary Fig. 4**). Notably, increased oxidative phosphorylation has been associated with the increased accumulation of MDR^{hi}/MG^{int-hi} cells, and thus this observation is consistent with *in vivo* phenotypes observed with Foxo1-ADA expressing CAR T cells (65). Collectively, our data suggests that overexpression of Foxo1-ADA in CAR T cells contributes to enhanced *in vivo* anti-tumor activity by promoting T cell polyfunctionality, proliferation and mitochondrial biogenesis to support effector functions.

As Foxo1, Id3 and Tcf7 contribute to the formation of memory T cells that home to secondary lymphoid tissues, we investigated whether CAR T cells overexpressing transcriptional regulators would exhibit enhanced trafficking to tumor draining lymph nodes (dLNs). Indeed, enumeration of $CD8^+$ CAR T cells within dLNs revealed that the overexpression of each of these factors increased the number of CAR T cells residing in tumor dLN relative to control CAR T cells (**Fig. 3g**). This was also associated with an increased presence of T_{SCM}-like ($CXCR3^+CD62L^+$) cells relative to control CAR T cells (**Fig. 3h**). Interestingly, a more comprehensive analysis of the relationship between Foxo1-ADA overexpression and the number of CAR T cells within draining lymph nodes revealed that Foxo1-ADA specifically enhanced the number of CAR T cells at the draining lymph nodes but not the non-draining lymph node from the opposite flank (**Fig. 3i**). This suggests that Foxo1-ADA expression specifically enhanced the migration and/or expansion of CAR T cells at the draining lymph node. To investigate the importance of dLN residency to the phenotype of Foxo1-ADA expressing CAR T cells, we correlated the number of dLN resident $CD8^+$ T cells to the frequency of intratumoral $IFN\gamma^+TNF^+$ cells in each treatment group and observed a significant positive correlation in mice treated with Tcf7 and Foxo1-ADA overexpressing CAR T cells (**Fig. 3j**). Collectively, our data infers that CAR T cell trafficking through tumor dLNs may be promoted through the overexpression of Foxo1-ADA and contributes to improved CAR T cell

polyfunctionality. Importantly, the increased therapeutic efficacy observed with Foxo1-ADA overexpressing CAR T cells was not associated with overt signs of toxicity (**Supplementary Fig. 2f-i**), highlighting the clinical potential of this approach.

Expression of wild-type FOXO1 enhances the stemness of human CAR T cells whilst enabling the acquisition of effector functionality upon activation

Having established the potential of Foxo1 overexpression in murine CAR T cells, we next investigated this in the context of human CAR T cells. Human T cells were transduced with an anti-Lewis Y CAR that is currently being used in a phase 1b clinical trial (NCT03851146) linked to FOXO1-ADA via a P2A peptide (**Supplementary Fig. 5a**). Strikingly, FOXO1-ADA overexpressing CAR T cells appeared less differentiated as indicated by an increased frequency of $CD62L^{+}CD27^{+}$ cells and $CD45RA^{+}$ cells concomitant with reduced expression of the exhaustion markers LAG3 and TIM3 (**Supplementary Fig. 5b-c**), a phenotype previously associated with improved CAR T cell responses in the clinic (13, 14, 66). However, unlike the case with murine CAR T cells, FOXO1-ADA overexpression appeared to prevent human CAR T cells from acquiring an effector-like phenotype after activation. Although FOXO1-ADA overexpressing CAR T cells significantly upregulated CD69 upon tumor cell coculture, (**Supplementary Fig. 5d**), their capacity to produce IFNγ and TNF was significantly attenuated relative to control CAR T cells (**Supplementary Fig. 5e**). This suggested that expression of constitutively active FOXO1 restricted the capacity of CAR T cells to gain full effector function and therefore led us to evaluate the overexpression of wild-type (WT) FOXO1 in human CAR T cells, which we hypothesized may result in a more stem like phenotype whilst enabling effective transition to effector like cells in response to antigen stimulation. Indeed, while overexpression of WT FOXO1 significantly enhanced the proportion of $CD45RA^{+}$ and $CD62L^{+}CD27^{+}$ CAR T cells (**Fig. 4a**), in contrast to FOXO1-ADA expressing CAR T cells, WT FOXO1-expressing CAR T cells were able to produce comparable levels of IFNγ and TNF to control CAR T cells upon coculture with tumor cells (**Supplementary Fig. 5e**). Given the phenotypic differences observed between the murine and human systems following overexpression of the constitutively active variant of FOXO1, we investigated whether this was due to differences in expression levels of the transgene between the two models. Indeed, overexpression of FOXO1 in human CAR T cells was more pronounced relative to murine counterparts with approximately a 5- and 2-fold increase in human FOXO1/ murine *Foxo1* mRNA respectively (**Supplementary Fig. 1b-c**). To determine whether these differences

accounted for the differences in phenotype we modified the human lentiviral vector such that expression was driven by a PGK or CMV promoter, both of which have been reported to give lower transgene expression relative to the EF1α promoter (67). In our hands the CMV promoter drove a significantly lower level of mCherry or FOXO1 expression relative to the EF1α and PGK promoters (**Supplementary Fig. 5f**) enabling us to evaluate the impact of high or low FOXO1 gene expression on CAR T cell phenotype. Whilst FOXO1-ADA was able to induce an increase in the $CD45RA^{+}CD62L^{+}$ population when driven by the EF1α, PGK or CMV promoters, the phenotype evoked by wild type FOXO1 was dependent on promoter strength with only a mild phenotype observed using the weak CMV promoter (**Supplementary Fig. 5g-h**). However, FOXO1-ADA significantly attenuated the production of IFNγ and TNF by CAR T cells regardless of the promoter used to drive its expression (**Supplementary Fig. 5i**). Given these results we decided to proceed with evaluation of the impact of FOXO1 WT expression driven by the EF1α promoter.

We next compared the impact of WT FOXO1, TCF7 and ID3 on the phenotype of anti-Lewis Y CAR T cells. FOXO1 was significantly more effective in the induction of the $CD45RA^{+}CD62L^{+}$ population of $CD8^{+}$ CAR T cells relative to TCF7 and ID3 (**Fig. 4b**) and indeed the increased proportion of $CD45RA^{+}CD62L^{+}$ cells following FOXO1 expression was reproducible across multiple donors (**Fig 4c**). WT FOXO1 overexpression was also associated with increased expression of CCR7 and CX3CR1 and reduced expression of activation/ exhaustion markers CD39, TIM3 and PD-1 (**Fig. 4d, Supplementary Fig. 6a**) and in the context of serial cocultures with OVCAR-3 or MCF7 tumor cells, WT FOXO1 overexpression led to a significant increase in the recovery of $CD8^{+}$ and $CD4^{+}$ CAR T cells, and were able to produce IFNγ and TNF levels comparable to control CAR T cells (**Supplementary Fig. 6b-c**). Phenotypic analysis of cell surface phenotype of WT FOXO1 overexpressing and control CAR T cells following coculture with tumor cells revealed a similar expression of PD-1 and TIM-3, but reduced expression of CD39 relative to control CAR T cells (**Supplementary Fig. 6d-e**). Notably, the reduced expression of CD39 mediated by FOXO1 was not recapitulated by the overexpression of either TCF7 or ID3 either in T cell only cultures (**Fig. 4b**) or following tumor cell coculture (**Supplementary Fig. 6f**), providing further evidence for an enhanced capacity of FOXO1 to favorably modulate CAR T cell phenotype relative to these factors. These observations are consistent with the notion that the overexpression of WT FOXO1 enabled the acquisition of a more stem-like phenotype that protects CAR T cells from exhaustion without

preventing the acquisition of effector function. In reverse experiments, CRISPR/Cas9 mediated targeting of FOXO1 in human anti-Lewis Y (LeY) CAR T cells led to a loss of CD62L expression and a reduction in CAR T cell expansion upon extended culture (**Supplementary Fig. 7a-d**). Moreover, FOXO1 deficient CAR T cells exhibited significantly impaired production of IFNγ upon coculture with LeY^+ OVCAR-3 or MCF7 tumor cells (**Supplementary Fig. 7e**). Given that phenotypic changes in FOXO1 expressing CAR T cells were largely reversible upon CAR T cell activation, we interrogated whether FOXO1 expressing CAR T cells could recover a more stem like phenotype after transient activation and recovery or in long-term chronic stimulation assays. Indeed, after activation followed by 1 week of rest FOXO1 expressing CAR T cells maintained higher level of $CD45RA^+CD62L^+$ (naïve) and $CD45RA^-CD62L^+$ (central memory) CAR T cells relative to controls (**Supplementary Fig. 8a**). Similarly, when control or FOXO1-expressing CAR T cells were exposed to tumor cells over a period of 3 weeks FOXO1 CAR T cells maintained an enriched proportion of $CD45RA^+CD62L^+$ CAR T cells as well as reduced expression of TIM3 and CD39 (**Supplementary Fig. 8b**).

Transcriptome analysis of FOXO1 expressing CAR T cells indicate profound changes to T cell differentiation and metabolism that are reversible upon activation.

To further understand the mechanisms underlying the more "stem-like" phenotype of FOXO1-expressng CAR T cells, RNA-Seq was performed on $CD8^+$ and $CD4^+$ CAR T cells. As expected, this analysis revealed that FOXO1 overexpressing $CD8^+$ CAR T cells exhibited increased expression of genes associated with less differentiated T cells relative to their control counterparts (**Fig. 4e**). This effect was significantly more pronounced than observed following TCF7 overexpression, confirming that FOXO1 instigated a broad transcriptional program that enhanced the stem-like state of CAR T cells (**Supplementary Fig. 6g).** Moreover, WT FOXO1 overexpressing $CD8^+$ CAR T cells exhibited decreased expression of immune checkpoints relative to control counterparts and this effect was also more marked than with TCF7 expressing CAR T cells (**Supplementary Fig. 6h-i**). Given our previous observations of improved mitochondrial fitness in murine Foxo1-ADA overexpressing CAR T cells, we assessed the impact of WT FOXO1 overexpression on genes associated with metabolic pathways both prior to and after overnight coculture with MCF7 tumor cells. In the steady state, both $CD8^+$ and to a lesser extent $CD4^+$ WT FOXO1 overexpressing CAR T cells

exhibited reduced expression of glycolytic genes, consistent with a more stem-like phenotype and as observed with IL-15 cultured CAR T cells. Interestingly however, we observed a switch in this phenotype after activation whereby FOXO1 overexpressing $CD8^+$ CAR T cells exhibited higher expression of glycolytic genes relative to control CAR T cells following coculture with Lewis Y^+ tumor cells (**Fig. 4f, Supplementary Fig. 6j**). Indeed, we observed that after activation the number of genes that were significantly different between control and FOXO1 expressing CAR T cells was significantly reduced, highlighting that expression of WT FOXO1 enabled the acquisition of a more stem like phenotype without preventing the acquisition of effector function (**Supplementary Fig. 6k).** To further investigate the metabolic phenotype of FOXO1 overexpressing CAR T cells, a Seahorse analysis was performed. FOXO1-expressing CAR T cells exhibited a significantly enhanced basal respiratory rate and maximal respiratory rate, with an increase in spare respiratory capacity also observed in 4/5 donors tested (**Fig. 4g**). Notably, there were minimal changes to these parameters in the context of TCF7 overexpressing CAR T cells, highlighting that FOXO1 overexpression was a superior strategy to enhance the metabolic fitness of CAR T cells (**Fig. 4h**).

Lastly, we utilized RNA-sequencing to address the question of whether FOXO1 overexpression could protect CAR T cells from exhaustion. In the steady state, we again observed that FOXO1 overexpression resulted in a significant negative enrichment of genes associated with exhaustion (68) relative to control CAR T cells, an effect that was not observed following TCF7 overexpression (**Supplementary Fig. 6l).** We next evaluated this in the context of stimulation and resting. In this repeat experiment, we again observed that prior to stimulation FOXO1-expressing CAR T cells exhibited reduced expression of exhaustion-related genes (**Supplementary Fig. 6m)**. Following stimulation through the CAR both control and FOXO1-expressing CAR T cells upregulated these genes such that there was no significant difference between the groups. However, after a period of rest, the negative enrichment for this gene set was restored in FOXO1 expressing CAR T cells, highlighting that these cells are protected from the transcription of genes associated with exhaustion.

To further understand the impact of FOXO1 overexpression on CAR T cell phenotype we performed scRNA-seq analyses on CAR T cells prior to and after coculture with MCF7 tumor cells. Unbiased clustering analysis confirmed that, consistent with the bulk RNA-sequencing data, there were significant differences between control and FOXO1-expressing CAR T cells but that these differences diminished after activation (**Supplementary Fig. 9a-b**). We therefore

further dissected our analysis into non-activated $CD8^+$ CAR T cells (**Fig. 4i**) and activated $CD8^+$ CAR T cells (**Fig. 4j**). This confirmed that FOXO1 expression enhanced the proportion of $CD8^+$ CAR T cells with a more 'stem-like' appearance, notably through the enrichment of a cluster (designated cluster 1) that was characterized by high expression of KLF2, SELL and IL7R (**Fig. 4i, Supplementary Fig. 9c**). This enhanced proportion of cluster 1 cells was offset by a reduction in the proportion of a cluster of cells (designated cluster 0) characterized by high expression of IFITM3 and TNFSF10 (**Supplementary Fig. 9c**). Indeed, comparing FOXO1 expressing CAR T cells within cluster 1 to control CAR T cells within cluster 0 revealed a significant enrichment for genes associated with less differentiated cells and reduced expression of genes associated with glycolysis and exhaustion, corroborating our results from bulk RNA-sequencing (**Fig. 4k**). Moreover, cluster 1 cells expressed high levels of CCR7, suggesting that these cells have the potential to traffic to lymph nodes, consistent with the phenotype observed with murine FOXO1-ADA expressing CAR T cells (**Fig. 4i**). Similar results were observed with non-activated $CD4^+$ T cells with enrichment of a cluster that exhibited high expression of SELL, KLF2 and IL7R (designated cluster 3) (**Supplementary Fig. 9b,d**). To further interrogate the phenotype of CAR T cells post activation, we repeated the analysis on only the activated cells. In this context, 6 distinct clusters of $CD8^+$ CAR T cells were observed. Though differences between control and FOXO1-expressing CAR T cells were less marked in than prior to activation this analysis did reveal an enrichment of a cluster (designated cluster 2) characterized by high expression of MKI67 and a concomitant decrease in cluster 5 (**Fig. 4j**). Comparison of the gene expression profiles of FOXO1-expressing cluster 2 cells and control cluster 5 cells we observed a positive enrichment for E2F target genes and glycolysis-related genes, suggesting that FOXO1-expressing CAR T cells are primed for a proliferative burst post activation (**Fig. 4l**) .

Foxo1 overexpression within CAR T cells imparts distinct epigenetic changes prior to antigen activation.

We next investigated the impact of FOXO1 expression on the epigenetic landscape of $CD8^+$ CAR T cells. FOXO1 overexpression led to dramatic changes with 3653 peaks with increased accessibility and 14335 peaks with decreased accessibility (**Fig. 5a**). In line with our observations of the impact of FOXO1 on the expression of immune checkpoints at both the protein and transcriptional level (**Fig. 4d, Supplementary Fig. 6e, h**), we observed that FOXO1 expression led to decreased accessibility at regions in proximity to the transcriptional start sites of genes encoding negative immune checkpoints such as PDCD1, ENTPD1 and

TIGIT (**Fig. 5b**). ChromVAR analysis revealed that regions that were significantly more accessible in FOXO1 expressing CAR T cells were enriched for motifs that included several other forkhead box family members, STAT1 and STAT3 and CTCF, a factor that has been shown to regulate $CD8^+$ T cell homeostasis through its interaction with TCF7 (69). Compared to control CAR T cells, FOXO1 overexpression strongly reduced the accessibility in regions containing motifs associated with AP-1 and NFκB subunit binding, in line with previous observations indicating that FOXO1 promotes a resting T cell state through repression of AP-1 activity (70) (**Fig. 5c**). Indeed, FOXO1 overexpression resulted in reduced expression of transcription factors previously observed to be upregulated in exhausted CAR T cells (71), including members of the AP-1 family such as IRF8 and FOSB (**Fig. 5d**). In line with our hypothesis that FOXO1 expression imparts a phenotype akin to IL-15 cultured cells, there was a clear correlation for motif accessibility between IL-15 cultured and FOXO1 expressing CAR T cells (**Fig. 5e**). Although FOXO1 implemented epigenetic changes consistent with reprogramming to a more stem-like phenotype, it did not prevent the acquisition of an effector-like epigenetic landscape post activation (**Fig. 5f**). Indeed, after stimulation through the CAR, FOXO1 overexpressing CAR T cells exhibited only 2533 sites with increased accessibility and 5217 with decreased accessibility relative to control CAR T cells, a decrease of ~30% and 65% respectively compared to prestimulated samples (**Fig. 5g**). The sites that exhibited reduced accessibility in resting FOXO1 expressing CAR T cells but not activated FOXO1 expressing CAR T cells (relative to control CAR T counterparts) were enriched in the promoter regions of genes at less than 1kb from the transcriptional start site (**Fig 5h**). Thus, accessibility to key effector genes such as IFNG, TNF and IL2 were similar in control and FOXO1 expressing cells after activation (**Fig. 5b**) and the decreased accessibility of sites of BATF:AP-1 motifs observed in resting FOXO1 expressing CAR T cells was no longer apparent after activation (**Fig. 5c**). Importantly, and consistent with our functional data, this suggests that WT FOXO1 expression promotes a stem like phenotype, but does not preclude epigenomic reprogramming required for T cell activation. Taken together, these *in vitro* observations highlighted the potential for FOXO1 overexpression to enhance the activity of human CAR T cells and led us to investigate this in the context of treatment of solid tumors.

FOXO1 expressing human CAR T cells exhibited improved anti-tumor efficacy.

To assess the *in vivo* efficacy of human FOXO1 expressing CAR T cells we evaluated their ability to control tumor growth in a human ovarian cancer model. To compare the impact of

TCF7, ID3 and FOXO1 overexpression *in vivo* we treated OVCAR-3 tumor bearing mice with CAR T cells expressing each transcription factor. Strikingly, FOXO1 was the only transcription factor that enhanced CAR T cell efficacy as indicated by a significant decrease in tumor weight (**Fig. 6a**), which was associated with a significant increase in the number of $CD8^+$ and $CD4^+$ CAR T cells in the blood and spleen of treated mice (**Fig. 6b-c**). Indeed, overexpression of FOXO1 significantly enhanced control of tumor growth relative to control CAR T cells (**Fig. 6d, Supplementary Fig. 10a**). Analysis of tumor-infiltrating CAR T cells revealed that FOXO1 overexpression significantly increased the proportion of $CD8^+$ and $CD4^+$ CAR T cells in the tumors of treated mice at day 12 post-treatment (**Fig. 6e**). In both tumors and spleens WT FOXO1 overexpressing $CD8^+$ CAR T cells exhibited a less differentiated phenotype (**Fig. 6f-g**). Tumor-infiltrating FOXO1 overexpressing $CD8^+$ CAR T cells also exhibited reduced expression of the exhaustion markers PD-1 and TIM3 relative to control CAR T cells but exhibited a similar proliferative capacity as indicated by Ki-67 expression (**Fig. 6h, Supplementary Fig. 10b**). Notably, these phenotypic differences were not observed following TCF7 overexpression, confirming the enhanced capacity of FOXO1 to favorably modulate CAR T cell phenotype and function (**Supplementary Fig. 10c-d**). Enhanced infiltration of WT FOXO1 overexpressing CAR T cells was also observed at day 7 post-treatment, when control CAR T cells were almost absent from the tumor site (**Supplementary Fig. 10e**). This was despite the fact that the frequency of FOXO1-expressing CAR T cells was not increased in the spleen at this timepoint, inferring that FOXO1-expressing CAR T cells had an advantage to traffic to the tumor site (**Supplementary Fig. 10f**). Analysis of serum from mice treated with control and FOXO1-expressing CAR T cells indicated no significant changes in the levels of enzymes associated with liver and kidney function (**Supplementary Fig. 10g**), or cytokines associated with cytokine release syndrome (**Supplementary Fig. 10h**). Moreover, treated mice elicited no significant changes in body weight during therapy supporting the safety of this approach **(Supplementary Fig. 10i)**. Finally, we evaluated this approach in the context of patient-derived CAR T cells using T cells derived from the initial apheresis product derived from six solid cancer patients who underwent anti-Lewis Y CAR T cell therapy. FOXO1 overexpression resulted in an increased population of $CD45RA^+CD62L^+$ stem-like T cells and reduced expression of TIM3 and CD39 **(Fig. 6i-j)**. Consistent with healthy donor derived CAR T cells, overexpression of FOXO1 in patient-derived CAR T cells led to a significantly enhanced maximal respiratory rate and spare respiratory capacity **(Fig. 6k).** To confirm that FOXO1 overexpression could modify CAR T cell phenotype and function *in vivo,* we treated OVCAR-3 tumor bearing mice with CAR T cells derived from 2 individual patients. In both

767 cases, FOXO1 expression in patient-derived CAR T cells significantly enhanced the numbers
768 of CAR T cells in both the spleens and tumors of treated mice (**Fig. 6l**). Importantly, these
769 CAR T cells also exhibited an increased proportion of $CD45RA^{+}CD62L^{+}$ "stem like"
770 phenotype in the spleen (**Fig. 6m**) and a less exhausted phenotype in the tumors characterized
771 by reduced expression of PD-1 and TIM-3 (**Fig. 6n**), indicating that that FOXO1
772 overexpression can similarly modulate patient derived CAR T cells towards a less
773 differentiated state.

Discussion

CAR T cells are now established as an effective therapy for the treatment of a number of hematological malignancies. Patient responses in these indications is correlated with a CAR T cell product with a less differentiated phenotype and an ability to achieve long-term persistence, providing long-term anti-tumor effects and protection (19, 66). However, challenges remain in the solid tumor context including CAR T cell exhaustion, terminal differentiation and an immunosuppressive tumor microenvironment that limits CAR T cell effector functions and metabolic dysfunction. A number of approaches to address these challenges are in pre-clinical and clinical development including combining CAR T cell therapy with immune checkpoint blockade, agonistic co-stimulatory antibodies and antagonism of suppression pathways (72). Furthermore, a number of studies have explored mechanisms to enable CAR T cells to adopt less differentiated phenotypes such as the use of the homeostatic cytokine IL-15 or small molecule inhibitors e.g. AKT inhibitors (73), PI3Ki (NCT03274219), or epigenetic modifiers e.g. JQ1 (22) to maintain CAR T cells in culture prior to transfer. Notably, AKT inhibition was shown to enhance the localization of FOXO1 to the nucleus and result in the upregulation of FOXO1 target genes. However, whilst small molecule inhibitors such as AKTi can be applied easily to CAR T cells in culture, the disadvantage for such approaches is that the effect on phenotype is transient such that once the CAR T cells are infused into the patient the CAR T cells differentiate and exhaust in a normal manner. Therefore, a gene engineering approach to improve CAR T cell resistance to exhaustion may be preferable. Although many genetic engineering approaches have been tested to enhance CAR T cell function, notably including the overexpression of the AP-1 factor c-Jun, there are few approaches that have sought to modulate CAR T cell metabolic activity (6, 20, 24, 74). In this study, we set out to identify transcriptional regulators that are central to the less differentiated and improved metabolic fitness of IL-15 preconditioned CAR T cells. Transcriptional regulator candidates were subsequently tested in a syngeneic immunocompetent setting against a solid tumor antigen. Foxo1 stood out as a major candidate of interest based on the significant enrichment of FOXO1 target genes in IL-15 cultured CAR T cells (48, 49). We therefore selected Foxo1-ADA as a primary candidate, which was benchmarked against Tcf7, Id3 and c-Jun overexpressing CAR T cells. Tcf7, Id3 and Foxo1 each contribute to T cell memory formation and generation of less differentiated T cell phenotypes (2, 47, 75). Such factors also promote T cell activity in chronic stimulation settings and contribute to the formation of precursor to exhausted T cells (T_{PEX}) that provide the proliferative burst of T cells in responses to immune checkpoint blockade (7, 48, 49, 76-78).

In line with our hypothesis, overexpression of these transcriptional regulators enhanced murine CAR T cell polyfunctionality as indicated by increased secretion of inflammatory cytokines and expression of GzmB. Notably, Foxo1-ADA was the most effective transcription factor at eliciting these phenotypes *in vivo*. Furthermore, despite enhanced, effector-like functions, CAR T cells overexpressing Foxo1-ADA maintained enhanced survival relative to control CAR T cells and retained a population of less differentiated $CD62L^{+}Ly108^{+}$ cells. Importantly, this indicates that increased cytokine production was not at the expense of less-differentiated cells, which would be detrimental to long-term persistence of CAR T cells.

Our *in vivo* therapeutic data demonstrated that Foxo1-ADA overexpression could significantly enhance CAR T cell mediated tumor regression in both the E0771-Her2 mammary fat pad model and subcutaneous MC38-Her2 colon carcinoma model. We concurrently observed that intratumoral Foxo1-ADA and Tcf7 overexpressing CAR T cells maintained higher frequencies of cells with a high mitochondrial mass and a functional mitochondrial membrane potential. Such a phenotype is important in supporting CAR T cell polyfunctionality and persistence and may have contributed to the production of IFNγ and TNF positive CAR T cells we observed intratumorally (17-19, 79).

Interestingly, we observed increased CAR T cell numbers within the dLNs of treated mice when overexpressing Foxo1-ADA or other memory associated transcriptional regulators. This is consistent with the roles of Foxo1, Tcf7 and Id3 in the formation of lymphoid tissue resident and circulating memory T cells. Thus, the promotion of less differentiated phenotypes may have enabled CAR T cells to traffic and localize to tumor dLNs (6, 46, 47, 52). This observation was particularly striking as control CAR T cells had little to no tumor dLN localization. Lymph node residency of Foxo1-ADA CAR T cells correlated to the increased frequency of IFNγ and TNF positive intratumoral CAR T cells, suggesting that lymph node residency may play a previously unappreciated role in maintaining CAR T cell polyfunctionality. This is of interest due to recent data indicating that the dLN is a key site for the maintenance of precursor exhausted T cells and response to immune checkpoint blockade (80). Moreover, the draining lymph nodes were identified as a key site in the mechanism by which an mRNA vaccine strategy enhanced CAR T cell responses (81). It therefore follows that a lack of lymph node residence observed for control CAR T cells may contribute to their dysfunction in solid tumor setting and that engineering strategies that result in draining lymph node residency may lead to

842 improved CAR T functionality. Whilst lymph node residency may have contributed to the
843 improved metabolic phenotype of Foxo1-ADA expressing CAR T cells *in vivo*, there are
844 clearly cell autonomous effects of FOXO1 overexpression since RNA-sequencing on control
845 and Foxo1-ADA overexpressing CAR T cells *in vitro* revealed an enrichment of oxidative
846 phosphorylation related genes, and decreased expression of glycolytic enzymes, prior to
847 activation. This was further supported by Seahorse analysis of human FOXO1 overexpressing
848 CAR T cells that revealed a significantly enhanced basal and maximal respiratory capacity,
849 consistent with our *in vivo* flow analyses of Foxo1-ADA expressing murine CAR T cells.
850
851 To demonstrate the feasibility of translating our findings to a clinical context, we overexpressed
852 a FOXO1-ADA human analogue in human LeY directed second generation CAR T cells.
853 Consistent with our murine data, we observed that human CAR T cells overexpressing
854 FOXO1-ADA appeared significantly less differentiated relative to control CAR T cells as
855 indicated by an upregulation of the memory marker CD62L and downregulation of the terminal
856 differentiation marker LAG3. However, unlike with murine CAR T cells, FOXO1-ADA
857 expression significantly prevented the acquisition of effector functions in CAR T cells
858 following recognition of their target antigen, almost completely abrogating their production of
859 proinflammatory cytokines. The reasons for these species differences are not fully known but
860 could potentially be related to differences in FOXO1 expression levels. In the human CAR T
861 cell system, we used the EF1α promoter system to drive FOXO1(ADA) expression, which led
862 to higher levels of overexpression than in the murine CAR T cell system. Indeed, whilst wild
863 type FOXO1 was able to promote the emergence of a less differentiated $CD45RA^{+}CD62L^{+}$
864 phenotype when expressed at high levels by the EF1α promoter, this effect was not observed
865 when using the weaker CMV promoter. These data highlight the importance of the strength of
866 transcription factor expression. Whilst expression of FOXO1-ADA prevented human CAR T
867 cells from acquiring effector functionality such as cytokine production, overexpression of WT
868 FOXO1 appeared to achieve a 'goldilocks' situation where a less differentiated phenotype can
869 be maintained in the steady state but robust effector cell differentiation can still be achieved
870 once the CAR becomes activated, as reflected by the fact that the majority of epigenetic and
871 transcriptional changes enforced by FOXO1 were reversible upon stimulation though the CAR.
872 In this regard, wildtype FOXO1 appears to exhibit favorable metabolic characteristics given
873 that FOXO1-expressing cells exhibit reduced expression of glycolysis related genes in the
874 steady state but can strongly upregulate these pathways upon activation. Overexpression of
875 wildtype FOXO1 in human CAR T cells led to significantly enhanced tumor regression in mice

similarly to that found with Foxo1-ADA overexpressing murine CAR T cells. This was associated with increased tumor infiltration of FOXO1 human CAR T cells and without overt signs of toxicity, supporting the safety and potential clinical applicability of this approach. Notably, in the context of human CAR T cells we observed that FOXO1 was significantly more able to promote the emergence of $CD45RA^{+}CD62L^{+}$ cells relative to TCF7 and ID3 and was the only transcription factor that enhanced the efficacy of CAR T cells in the xenograft setting. Further comparison between FOXO1- and TCF7- overexpressing CAR T cells revealed that FOXO1 was unique in its ability to favorably modulate metabolic function and was significantly more able to drive transcriptional changes consistent with a more persistent and less exhausted CAR T cell product. To further understand the mechanism underlying this, scRNAseq analysis was performed, which indicated that FOXO1 expression promoted the emergence of a sub-population of $CD8^{+}$CAR T cells characterized by high expression of CD62L, IL7R and KLF2. This population appeared largely responsible for the gene signatures of reduced exhaustion/ glycolysis and also notably expressed high levels of CCR7, suggesting that our observations of increased lymph node residency may also be reflected in human CAR T cells engineered to express FOXO1.

Whilst clinical trials assessing the use of the IL-15 signaling to generate less differentiated CAR T cells are ongoing (NCT05359211, NCT05103631, NCT04715191, NCT04377932, NCT03721068, NCT02992834), such effects are only transient and fail to provide long term protection against exhaustion once CAR T cells become chronically stimulated in the solid TME. Our study presents as a more durable approach maintaining CAR T cell fitness and persistence whilst promoting polyfunctionality and anti-tumor efficacy without evidence of toxicity. Furthermore, as our study suggests that murine Foxo1-ADA overexpressing CAR T cells are able to acquire effector functions and synergize with immune checkpoint blockade therapies including anti-PD-1, there is also a high potential for human FOXO1 overexpressing CAR T cells to synergize with these existing therapies to further enhance anti-tumor potential (82). Therefore, our study holds broad clinical potential for enhancing CAR T cell efficacy in solid cancers.

Acknowledgments.

The authors wish to acknowledge the Peter MacCallum Molecular Genomics Core for their assistance in designing and performing transcriptomic and epigenetic sequencing experiments.

Figure Legends

Figure 1. CAR T cells polarized with IL-15 have increased expression of Foxo1

a, Murine anti-Her2 $CD8^+$ CAR T cell expression of CD44 and CD62L following preconditioning with IL-2 and IL-7 or IL-15 and IL-7. **b,** CAR T cell numbers from tumors and spleens of E0771-Her2 tumor bearing mice at day 9 post treatment following preconditioning with indicated cytokines. **c-e,** Heatmaps and MA-plot of indicated transcriptional regulators or glycolytic enzymes in $CD8^+CD62L^+$ CAR T cells cultured *in vitro* with indicated cytokines at day 6 post transduction. **f-g**. Gene set enrichment analyses of CAR T cells from **c.** relative to the CHEA dataset (**f**) and *in silico* predicted FOXO1 target genes (**g;** FOXO_01; https://www.gsea-msigdb.org/gsea/msigdb/cards/FOXO1_01.html). **h-j**. $CD8^+$ CAR T cells treated as per **c.** were analyzed by ATAC-Seq. **h-i,** Homer analysis of motif enrichment in differentially accessible peaks. The top 50 most significantly enriched motifs in IL-15 conditioned CAR T cells are plotted relative to the percentage of target sequence and average expression in IL-15 cultured $CD8^+CD62L^+$ CAR T cells. **j,** ChromVar analysis of cells from **h.** Mean deviation score was calculated for the following subsets of $CD8^+$ CAR T cells; cultured in either IL-2 and IL-7 or IL-7 and IL-15; $CD62L^+CD44^+$, $CD62L^+CD44^{low}$, $CD62L^-CD44^+$. The delta mean deviation score for the $CD62L^+CD44^+$ subset cultured in IL-2/IL-7 or IL-7/IL-15 is shown for the top 10 ranking transcription factors in each direction. **k-l.** anti-Her2 CAR T cells were CRISPR/Cas9-edited to target *Foxo1*. At day 5 post transduction $CD8^+$ CAR T cells were phenotyped for expression of CD62L and Tcf1 in steady state (**k**) or serially cocultured with E0771-Her2 tumor cells for 3 consecutive days and expression of indicated markers determined (**l-m**). **a** and **k-m** representative of >3 independent experiments, data points indicate biological triplicates, **b,** n= 7 mice per group. Bars represent mean ± s.e.m, (**p<0.01). **c-j** Samples indicative of biological duplicates.

Figure 2. Foxo1-ADA overexpression enhances CAR T cell survival, polyfunctionality and therapeutic activity

a, Schematic of tumor cell coculture assay. **b,** IFNγ and TNF production following each round of E0771-Her2 tumor cell stimulation with CAR T cells modified via overexpression of indicated transcription factors. **c**. Paired analyses of n = 4 repeat experiments setup as per **b.** **d-e,** Expression of Granzyme B in CAR T cells following 72 hours of coculture. **f,** Number of total or $CD62L^+Ly108^+$ $CD8^+$ CAR T cells. Bars represent mean ± SD of triplicate samples

from a representative experiment of n = 3. Histogram overlays concatenated from biological replicates. **g,** schematic for *in vivo* experiments, **h-i** Treatment of subcutaneous MC38-Her2 or mammary fat pad E0771-Her2 tumors. Tumors were established in mice for 5 to 7 days, prior to treatment with two doses of 1 x 10^7 indicated CAR T cells administered on subsequent days. **b,** and **e-f** one-way ANOVA, representative of at least 3 independent experiments. **c,** paired Student's T test, (**p <0.01, ***p < 0.001, ****p < 0.0001). **h-i,** Tumor growth represented as mean tumor size from n = 15-18 mice per group ± SEM from 3 pooled experiments. Two-way ANOVA. (**p <0.01, ****p < 0.0001).

Figure 3. Foxo1-ADA overexpression enhances *in vivo* polyfunctionality and metabolic fitness

a-d, Flow cytometry analysis of tumor infiltrating CAR T cells from mice bearing E0771-Her2 mammary fat pad tumors at 9-days post treatment. **a,** Frequency of tumor infiltrating $CD8^+$ CAR T cells expressing IFNγ and TNF. Left panel- concatenated samples from one experiment, right panel- data from individual mice. **b,** Frequency of intratumoral CAR T cells expressing 0, 1, 2 or 3 effector proteins of IFNγ, TNF and GzmB. **c,** MC38-Her2 tumor growth in mice treated as per **Figure 2**. Where indicated mice were co-treated with anti-IFNγ (H22; 250 µg per mouse) at days -1, 0 and 7 post treatment. **d-e,** Mitotracker Deep Red (MDR) and Mitotracker Green (MG) staining tumor infiltrating $CD8^+$ CAR T cells. **d**, staining of concatenated samples **e,** MDR and MG staining intensity for individual mouse replicates. **f,** Heatmap for genes in the oxidative phosphorylation Hallmark pathway $CD8^+$ CAR T cells at 72 hours post anti-CAR stimulation. **g-j,** Flow cytometry analysis of tumor, draining lymph node (dLN) on non-draining lymph node (ndLN) associated CAR T cells from mice bearing E0771-Her2 mammary fat pad tumors at 9-days post treatment. Number of total (**g**) or $CXCR3^+CD62L^+$ **(h)** tumor dLN resident CD8- CAR T cells. **i,** Paired analysis of number of CAR T cells in the ndLN and dLN. **j,** Correlation of number of tumor dLN resident $CD8^+$ CAR T cells to frequency of $IFN\gamma^+TNF^+$ intratumoral $CD8^+$ CAR T cells. **a-b, e-i** Bars represent mean ± SEM from indicated number of mice pooled from 2 independent experiments, One way ANOVA. **c.** Data represents the mean ± s.e.m of 3-5 mice per group, Two way ANOVA (*p<0.05, **p <0.01, ****p < 0.0001).

Figure 4. Human CAR T cells overexpressing FOXO1 are resistant to exhaustion and exhibit improved metabolic fitness

Anti-Lewis Y CAR T cells were generated via activation of human peripheral blood mononuclear cells (PBMCs) for 48 hours with IL-2 and OKT3 followed by lentiviral transduction, **a-d**, The impact of FOXO1, TCF7 or ID3 overexpression on CAR T cell phenotype was determined **a** and **d,** flow cytometry analysis for expression of indicated markers on $CD8^+CAR^+$ T cells. **b,** Left panel as per **(a).** Right panel indicates the proportion of CD8+ CAR T cells expressing a $CD45RA^+CD62L^+$ phenotype. Circles, squares and triangles represent 3 individual donors. Transcription factors are color coded. **c.** Paired analysis from 12 individual experiments. **e-f,** $CD8^+$ CAR T cells were analyzed by RNA-Seq before and after activation with MCF7 tumor cells. Data represented by biological triplicates. e**,** enrichment of genes associated with less differentiated T cells that correlate with improved responses to immune checkpoint blockade in FOXO1 expressing CAR T cells. Heatmap depicts the 38 genes with highest differential expression in the G10 memory cluster identified by Sade-Feldmann *et al.* **f,** expression of glycolysis related genes before and after coculture with MCF7 tumor cells. **g-h,** Analysis of CAR T cell oxidative consumption by Seahorse MitoStress assay following transduction with FOXO1 (**g**) or TCF7 (**h**). Data shown represents paired analysis from independent donors (top) or a representative donor (bottom). **i**-l Control or FOXO1-expressing CAR T cells were left non-stimulated or stimulated for 16 hours with MCF7 tumor cells and then analysed by scRNA-seq. **i-j** UMAP plots, cell cluster composition and density plots showing expression of indicated genes of of non-stimulated (**i**) and stimulated (**j**) $CD8^+$ CAR T cells. **k,** left- Visualization of gene signatures scores (SingleCellSignature) of memory, glycolysis and exhaustion gene-sets in unstimulated $CD8^+$ T cells right- Gene set enrichment analysis for indicated pathways comparing FOXO1 expressing CAR T cells within cluster 1 to control CAR T cells within cluster 0 (non-stimulated clusters). **l,** Gene set enrichment analysis for indicated pathways comparing FOXO1 expressing CAR T cells within cluster 2 to control CAR T cells within cluster 5 (stimulated clusters). Statistical significance determined by paired T test (**c, g, h**). * $p<0.05$, ** $p<0.01$, ***$p<0.001$, **** $p<0.0001$.

Figure 5. FOXO1 overexpression induces an epigenetic landscape that promotes CAR T cell stemness but does not preclude effector-like transition upon CAR T cell activation. FOXO1 or control CAR T cells were analyzed by ATACseq 7 days post generation either in the context of no stimulation or after 16 hour coculture with MCF7 tumor cells at a 1:1 ratio. $CD8^+$ CAR T cells were purified by FACS sorting prior to analysis. Experiment was performed in biological triplicates. **a,** Differential peak analysis of non-stimulated control or FOXO1-expressing CAR T cells. **b,** IgV tracks for indicated genes in named CAR T cell groups. **c,**

ChromVAR analysis of motifs (JASPAR) with increased or decreased accessibility in FOXO1-expressing CAR T cells. Heatmap depicts the top 20 motifs in each direction for non-stimulated cells and the same motifs after CAR activation. **d,** fold reduction in indicated transcription factor expression following FOXO1 overexpression in $CD8^+$ CAR T cells analyzed as per Fig 4e. **e,** Correlation of motifs with upregulated by IL-15 relative to IL-2 in murine CAR T cells as per Figure 1 and in FOXO1 overexpressing CAR T cells as determined by HOMER analysis. **f,** PCA of ATAC-seq data for indicated CAR T cell populations. **g,** Number of peaks with differential accessibility in FOXO1 expressing CAR T cells relative to controls before and after stimulation **h,** Location of peaks with reduced accessibility in FOXO1-expressing T cells relative to controls prior to stimulation (left) and after MCF7 coculture (right).

Figure 6. FOXO1 overexpression enhances human CAR T cell efficacy

a. OVCAR-3 tumor weights following 13 days treatment with CAR T cells expressing indicated transcription factor. **b-c**. Analysis of CAR T cell frequency in the blood (**b**) and spleens (**c**) of treated mice at day 12/ 13 post treatment. **a-c**. Data represents the mean ± SEM of 6 or 12 mice per group. **d.** Therapeutic efficacy of anti-Lewis Y CAR T cells utilized to treat mice bearing OVCAR-3 tumors. Data represents the mean ± SEM of 7 mice per group from a representative experiment of n = 2. **e-h.** Analysis of CAR T cell frequency and phenotype in the spleens and tumors of treated mice at day 12 post treatment. Data represents the mean ± SEM of 5 mice per group. **i,** Proportion of CD8+ T cells exhibiting a $CD45RA^+CD62L^+$ phenotype in $CD8^+$ CAR T cells generated from six patients enrolled onto a CAR T cell trial. **J,** Expression of TIM3 and CD39 on $CD8^+$ CAR T cells derived from patients. **k.** Analysis of patient-derived CAR T cell oxidative consumption by Seahorse MitoStress assay following transduction with FOXO1 **k**. Data shown represents paired analysis from independent donors (left) or a representative patient (right). **l-m** Analysis of CAR T cell frequency (**l**) and phenotype (**m**) in the spleens and tumors of mice treated with patient derived CAR T cells at day 13 post treatment. Data represents the mean ± SEM of 7-15 mice per group. Statistical significance determined by one way ANOVA (**a-c**), two way ANOVA (**d**), unpaired t test (**e, g, h, l, m**) or paired T test (**i, k**) * $p<0.05$.

Supplementary Figure 1. CAR T cell transduction efficiency and transgene overexpression

a, Schematic of anti-Her2 CAR with Myc binding domain and detection of this Myc tag in CAR T cells modified with the indicated transcription factors. Representative of more than 3

independent transductions. **b,** Expression of indicated transcription factors in murine $CD8^+NGFR^+$ (**b**) or human FACS sorted CAR T cells as determined by qRT-PCR**.** Data presented as mean ± SD. Unpaired Student's T test (*p<0.05, ***p <0.001, ****p < 0.0001).

Supplementary Figure 2. Therapeutic efficacy and safety of murine CAR T cells in E0771-Her2 and MC38-Her2 tumor bearing mice.

a-b MC38-Her2 subcutaneous tumors or **c,** E0771-Her2 mammary fat pad tumors were established in mice for 5 to 7 days, prior to treatment with control, Tcf7, Foxo1-ADA or Id3 overexpressing CAR T cells as per **Figure 2**. Survival (**a**) and individual tumor growth curves (**b-c**) of mice **a,** Mantel-Cox test, n = 11-12 mice per group *, p<0.05 **, p<0.01. **d-e**. Therapeutic efficacy of control, wild-type Foxo1 (Foxo1 WT) overexpressing, Foxo1-ADA overexpressing, c-Jun overexpressing or no CAR T cells. Data presented as mean ± SEM of n = 4-6 mice per group. Two-way ANOVA (ns = not significant, *p<0.05, **p <0.01, ***p<0.001). **f-h** At day 9 post treatment serum was taken from treated mice. Liver and kidney function was assessed by levels of indicated factors and potential cytokine release syndrome assessed through measurement of indicated cytokines. **i,** hematoxylin and eosin histology staining was performed on brain liver and lungs of mice day 9 post treatment.

Supplementary Figure 3. Phenotype of anti-Her2 CAR T cells isolated from E0771-Her2 expressing tumors

E0771-Her2 tumor bearing mice were treated with anti-Her2 CAR T cells and tumors analyzed by flow cytometry at day 9 post treatment. **a,** Proportion of $CD8^+$ **b,** or $CD8^+Tcf1^+$ CAR T cells expressing Ki67. **c,** Expression of PD-1, TIM-3 and Tox in $CD8^+$ CAR T cells modified with the indicated transcription factor. Data obtained from concatenated samples of n = 6 mice from a representative experiment of n = 2. **d,** E0771-Her2 tumor-bearing mice were treated with CAR T cells and a total of 4 doses of 200 µg of anti-PD-1 or 2A3 on days 0, 3, 7 and 11 post-treatment. Data presented as mean ± SEM of n = 5-6 mice per group. Two-way ANOVA (ns = not significant, *p<0.05). **e,** frequency of $CD8^+$ and $CD4^+$ T cells within the $NGFR^+$ (CAR^+ subset). Data represented as the mean ± SEM of n = 8-12 per group.

Supplementary Figure 4. GSEA pathways in *in vitro* stimulated Foxo1-ADA overexpressing CAR T cells

Foxo1-ADA and control CAR T cells were stimulated for 72 hours with an agonistic antibody against the Her2 directed CAR prior to RNA-sequencing. Unbiased ranking of gene sets from the Hallmark gene sets.

Supplementary Figure 5. Comparison of FOXO1 WT and FOXO1-ADA in human CAR T cells.

a, LeY-FOXO1-ADA and LeY-FOXO1 WT transgene structure. **b,** expression of indicated markers on healthy donor derived $CD8^+$ CAR T cells 5 days post transduction. **c,** Timecourse analysis of $CD8^+$ CAR T cell phenotypes during *in vitro* culture. **d-e**. CAR T cells were serially coculture with OVCAR-3 tumor cells through 3 successive rounds of tumor cell addition. **d,** Expression of CD69 following coculture. **e,** proportion of $CD8^+$ CAR T cells expressing IFNγ and TNF in control- FOXO1-ADA or FOXO1 WT expressing CAR T cells from a representative experiment of 3 independent donors. **f,** T cells were transduced with the anti-Lewis Y CAR and mCherry or FOXO1 WT transgenes driven by the EF1α, PGK or CMV promoters. Representative flow cytometry showing the expression of mCherry (left) or FOXO1 (right). Numbers indicate MFI for relevant transgenes. **g-h,** Flow cytometry analysis of the $CD45RA^+CD62L^+$ profile of $CD8^+$ CAR T cells transduced with either mCherry (Ctrl), FOXO1 WT or FOXO1-ADA driven by the indicated promoter. Representative plots (**g**) and paired data is shown for 3 independent donors (**h**). **i.** CAR T cells were cocultured for 24 hours with OVCAR-3 or MCF7 tumor cells and production of IFNγ and TNF determined. Data is represented as the mean ± SD of triplicate cultures. **d,** Unpaired T test. **e,** One-way ANOVA, **i**, unpaired t test. ****$p < 0.0001$.

Supplementary Figure 6. Phenotype and transcriptional profile of healthy donor CAR T cells following FOXO1 overexpression

Healthy donor T cells were transduced with mCherry (ctrl), FOXO1, TCF7 or ID3 and an anti-Lewis Y CAR. **a,** paired analysis of indicated phenotypic markers in control and FOXO1 expressing CAR T cells. Statistical significance determined by paired t test * $p< 0.05$. **b-f,** CAR T cells were serially cocultured with OVCAR-3 or MCF7 tumor cells over 72 hours after which point CAR T cell number (**b**), cytokine production (**c**) or cell surface phenotype (**d-f**) were determined. Data represents the mean ± SD of biological triplicates from a representative experiment of n = 4 (**d-e**) or n = 2 (**f**). 8< **g-l**. Gene expression of $CD8^+$ CAR T cells (**g-i, k**) and $CD4^+$ CAR T cells (**j-k**) was determined by RNA-Sequencing as per **Figure 4.** Data

indicative of biological triplicates.. **g,** enrichment of genes associated with less differentiated T cells that correlate with improved responses to immune checkpoint blockade in FOXO1- but not TCF7 expressing CAR T cells. **h-i,** Expression of indicated immune checkpoints in control, TCF7- or FOXO1 expressing $CD8^+$ CAR T cells **j,** Expression of genes associated with glycolysis. **k,** Volcano plot highlighting differentially expressed genes in control or FOXO1-expressing CAR T cells prior to and after tumor cell coculture. **l,** negative enrichment of genes associated with exhaustion in FOXO1-expressing but not TCF7-expressing CD8+ CAR T cells, gene set defined by (68) . **m,** Control or FOXO1-expressing $CD8^+$ CAR T cells were assessed by RNA-Sequencing prior to stimulation (left), after 24 hours activation with 0.1 µg/ml plate bound anti-Lewis Y (middle) or after 7 days recovery post stimulation with anti-Lewis Y (right).

Supplementary Figure 7. Phenotype and function of anti-Lewis Y CAR T cells following CRISPR/Cas9-mediated deletion of FOXO1.

anti-Lewis Y CAR T cells deficient for FOXO1 were generated via CRISPR/Cas9 targeting. The expression of CD62L and CD27 by $CD8^+CAR^+$ T cells (**a-b**) and $CD4^+CAR^+$ T cells (**c-d**) were determined over 28 days in culture with IL-2. **b, d,** Numbers of total (left) or $CD27^+CD62L^+$ (right) CAR T cells. **e,** CAR T cells were cocultured overnight at a 1:1 ratio with OVCAR-3 or MCF7 tumor cells for 16 hours and the production of IFNγ or TNF determined by CBA**.** Statistical significance determined by unpaired t test. *p<0.05, **p<0.01, ***p<0.001, ****p<0.0001.

Supplementary Figure 8. Phenotype of human CAR T cells expressing WT FOXO1 following repetitive stimulation cocultures.

a, CAR T cells were stimulated as per **Supplementary Fig. 6m**. Expression of CD45RA and CD62L on $CD8^+$ CAR T cells is shown for a representative donor n = 3. **b,** CAR T cells were stimulated with MCF7 Cancer cells for three weeks and the phenotype determined. Flow cytometry plots from a representative donor of n=2.

Supplementary Figure 9. scRNA-seq analysis of control and FOXO1-expressing CAR T cells.

CAR T cells were either left non stimulated or cocultured with MCF7 tumor cells and analyzed by scRNA-Seq as per **Fig. 4i. a-b,** UMAP plots, cluster composition and density plot of

indicated genes shown for pooled stimulated and non-stimulated $CD8^+$ (**a**) and $CD4^+$ (**b**) CAR T cells. **c-d,** Heatmap indicating the expression of the top 10 differentially expressed genes in each (**c**) $CD8^+$ and (**d**) $CD4^+$ cluster.

Supplementary Figure 10. Phenotype and safety of FOXO1-expressing ant-Lewis Y CAR T cells *in vivo*

OVCAR tumor bearing mice were treated with control, FOXO1- or TCF7-expressing CAR T cells. a. Individual tumor growth curves for mice treated in **Fig. 6d. b,** Analysis of expression of Ki-67 by $CD8^+$ CAR T cells in the tumors of treated mice at day 12. **c-d,** Expression of PD-1 and TIM3 in the tumor and CD45RA and CD62L in the spleens of treated mice at day 12 post treatment. **c,** representative FACS staining from concatenated samples. **d,** data represented as the mean ± SEM of n = 6 or 12 per group**. e, f,** Analysis of CAR T cell frequency in the tumors (**e**) and spleens (**f**) of treated mice at day 7 post treatment. **g,** analysis of enzyme concentrations and g, cytokines within the sera of treated mice at day 12 post treatment. **h,** body weight of mice at day 19, experimental endpoint of **Figure 4d**. Statistics determined by one way ANOVA (**c**) or unpaired t test (**e-f**) *$p<0.05$, ****$p<0.0001$.

References

1. Maude SL, Frey N, Shaw PA, Aplenc R, Barrett DM, Bunin NJ, et al. Chimeric antigen receptor T cells for sustained remissions in leukemia. N Engl J Med. 2014;371(16):1507-17.
2. Kochenderfer JN, Dudley ME, Feldman SA, Wilson WH, Spaner DE, Maric I, et al. B-cell depletion and remissions of malignancy along with cytokine-associated toxicity in a clinical trial of anti-CD19 chimeric-antigen-receptor–transduced T cells. Blood. 2012;119(12):2709-20.
3. Kalos M, Levine BL, Porter DL, Katz S, Grupp SA, Bagg A, et al. T Cells with Chimeric Antigen Receptors Have Potent Antitumor Effects and Can Establish Memory in Patients with Advanced Leukemia. Science Translational Medicine. 2011;3(95):95ra73-95ra73.
4. Mardiana S, Solomon BJ, Darcy PK, Beavis PA. Supercharging adoptive T cell therapy to overcome solid tumor–induced immunosuppression. Science Translational Medicine. 2019;11(495):eaaw2293.
5. Yang JC, Rosenberg SA. Adoptive T-Cell Therapy for Cancer. Advances in immunology. 2016;130:279-94.
6. Blank CU, Haining WN, Held W, Hogan PG, Kallies A, Lugli E, et al. Defining 'T cell exhaustion'. Nature Reviews Immunology. 2019;19(11):665-74.
7. Kallies A, Zehn D, Utzschneider DT. Precursor exhausted T cells: key to successful immunotherapy? Nature Reviews Immunology. 2020;20(2):128-36.
8. Giraldo NA, Becht E, Vano Y, Petitprez F, Lacroix L, Validire P, et al. Tumor-Infiltrating and Peripheral Blood T-cell Immunophenotypes Predict Early Relapse in Localized Clear Cell Renal Cell Carcinoma. Clinical Cancer Research. 2017;23(15):4416-28.
9. Ficial M, Jegede OA, Sant'Angelo M, Hou Y, Flaifel A, Pignon J-C, et al. Expression of T-Cell Exhaustion Molecules and Human Endogenous Retroviruses as Predictive Biomarkers for Response to Nivolumab in Metastatic Clear Cell Renal Cell Carcinoma. Clinical Cancer Research. 2021;27(5):1371-80.
10. Chan JD, Lai J, Slaney CY, Kallies A, Beavis PA, Darcy PK. Cellular networks controlling T cell persistence in adoptive cell therapy. Nature Reviews Immunology. 2021;21(12):769-84.
11. Klebanoff CA, Gattinoni L, Torabi-Parizi P, Kerstann K, Cardones AR, Finkelstein SE, et al. Central memory self/tumor-reactive CD8+ T cells confer superior antitumor immunity compared with effector memory T cells. Proceedings of the National Academy of Sciences of the United States of America. 2005;102(27):9571-6.
12. Siddiqui I, Schaeuble K, Chennupati V, Fuertes Marraco SA, Calderon-Copete S, Pais Ferreira D, et al. Intratumoral Tcf1+PD-1+CD8+ T Cells with Stem-like Properties Promote Tumor Control in Response to Vaccination and Checkpoint Blockade Immunotherapy. Immunity. 2019;50(1):195-211.e10.
13. Guo Y, Feng K, Liu Y, Wu Z, Dai H, Yang Q, et al. Phase I Study of Chimeric Antigen Receptor-Modified T Cells in Patients with EGFR-Positive Advanced Biliary Tract Cancers. Clin Cancer Res. 2018;24(6):1277-86.
14. Fraietta JA, Lacey SF, Orlando EJ, Pruteanu-Malinici I, Gohil M, Lundh S, et al. Determinants of response and resistance to CD19 chimeric antigen receptor (CAR) T cell therapy of chronic lymphocytic leukemia. Nat Med. 2018;24(5):563-71.
15. Li F, Liu H, Zhang D, Ma Y, Zhu B. Metabolic plasticity and regulation of T cell exhaustion. Immunology. 2022;167(4):482-94.
16. Weber EW, Parker KR, Sotillo E, Lynn RC, Anbunathan H, Lattin J, et al. Transient rest restores functionality in exhausted CAR-T cells through epigenetic remodeling. Science. 2021;372(6537).

17. Hirabayashi K, Du H, Xu Y, Shou P, Zhou X, Fucá G, et al. Dual-targeting CAR-T cells with optimal co-stimulation and metabolic fitness enhance antitumor activity and prevent escape in solid tumors. Nature Cancer. 2021;2(9):904-18.
18. van Bruggen JAC, Martens AWJ, Fraietta JA, Hofland T, Tonino SH, Eldering E, et al. Chronic lymphocytic leukemia cells impair mitochondrial fitness in CD8+ T cells and impede CAR T-cell efficacy. Blood. 2019;134(1):44-58.
19. Melenhorst JJ, Chen GM, Wang M, Porter DL, Chen C, Collins MA, et al. Decade-long leukaemia remissions with persistence of CD4+ CAR T cells. Nature. 2022;602(7897):503-9.
20. Seo H, González-Avalos E, Zhang W, Ramchandani P, Yang C, Lio C-WJ, et al. BATF and IRF4 cooperate to counter exhaustion in tumor-infiltrating CAR T cells. Nature Immunology. 2021;22(8):983-95.
21. Hurton LV, Singh H, Najjar AM, Switzer KC, Mi T, Maiti S, et al. Tethered IL-15 augments antitumor activity and promotes a stem-cell memory subset in tumor-specific T cells. Proceedings of the National Academy of Sciences. 2016;113(48):E7788-E97.
22. Kagoya Y, Nakatsugawa M, Yamashita Y, Ochi T, Guo T, Anczurowski M, et al. BET bromodomain inhibition enhances T cell persistence and function in adoptive immunotherapy models. The Journal of Clinical Investigation. 2016;126(9):3479-94.
23. Chow MT, Ozga AJ, Servis RL, Frederick DT, Lo JA, Fisher DE, et al. Intratumoral Activity of the CXCR3 Chemokine System Is Required for the Efficacy of Anti-PD-1 Therapy. Immunity. 2019;50(6):1498-512 e5.
24. Giuffrida L, Sek K, Henderson MA, House IG, Lai J, Chen AXY, et al. IL-15 Preconditioning Augments CAR T Cell Responses to Checkpoint Blockade for Improved Treatment of Solid Tumors. Molecular Therapy. 2020.
25. Alizadeh D, Wong RA, Yang X, Wang D, Pecoraro JR, Kuo CF, et al. IL15 Enhances CAR-T Cell Antitumor Activity by Reducing mTORC1 Activity and Preserving Their Stem Cell Memory Phenotype. Cancer Immunol Res. 2019;7(5):759-72.
26. Darcy PK, Haynes NM, Snook MB, Trapani JA, Cerruti L, Jane SM, et al. Redirected Perforin-Dependent Lysis of Colon Carcinoma by Ex Vivo Genetically Engineered CTL. The Journal of Immunology. 2000;164(7):3705-12.
27. Haynes NM, Snook MB, Trapani JA, Cerruti L, Jane SM, Smyth MJ, et al. Redirecting Mouse CTL Against Colon Carcinoma: Superior Signaling Efficacy of Single-Chain Variable Domain Chimeras Containing TCR-ζ vs FcεRI-γ. The Journal of Immunology. 2001;166(1):182-7.
28. Beavis PA, Henderson MA, Giuffrida L, Mills JK, Sek K, Cross RS, et al. Targeting the adenosine 2A receptor enhances chimeric antigen receptor T cell efficacy. J Clin Invest. 2017;127(3):929-41.
29. DeLuca DS, Levin JZ, Sivachenko A, Fennell T, Nazaire MD, Williams C, et al. RNA-SeQC: RNA-seq metrics for quality control and process optimization. Bioinformatics. 2012;28(11):1530-2.
30. Zerbino DR, Achuthan P, Akanni W, Amode MR, Barrell D, Bhai J, et al. Ensembl 2018. Nucleic Acids Res. 2018;46(D1):D754-D61.
31. Robinson MD, McCarthy DJ, Smyth GK. edgeR: a Bioconductor package for differential expression analysis of digital gene expression data. Bioinformatics. 2010;26(1):139-40.
32. McCarthy DJ, Chen Y, Smyth GK. Differential expression analysis of multifactor RNA-Seq experiments with respect to biological variation. Nucleic Acids Res. 2012;40(10):4288-97.
33. Korotkevich G, Sukhov V, Sergushichev A. Fast gene set enrichment analysis. bioRxiv. 2019:060012.

34. Subramanian A, Tamayo P, Mootha VK, Mukherjee S, Ebert BL, Gillette MA, et al. Gene set enrichment analysis: a knowledge-based approach for interpreting genome-wide expression profiles. Proc Natl Acad Sci U S A. 2005;102(43):15545-50.
35. Liberzon A, Subramanian A, Pinchback R, Thorvaldsdottir H, Tamayo P, Mesirov JP. Molecular signatures database (MSigDB) 3.0. Bioinformatics. 2011;27(12):1739-40.
36. Liberzon A, Birger C, Thorvaldsdottir H, Ghandi M, Mesirov JP, Tamayo P. The Molecular Signatures Database (MSigDB) hallmark gene set collection. Cell Syst. 2015;1(6):417-25.
37. Kanehisa M, Goto S. KEGG: kyoto encyclopedia of genes and genomes. Nucleic Acids Res. 2000;28(1):27-30.
38. Sade-Feldman M, Yizhak K, Bjorgaard SL, Ray JP, de Boer CG, Jenkins RW, et al. Defining T Cell States Associated with Response to Checkpoint Immunotherapy in Melanoma. Cell. 2019;176(1-2):404.
39. Pont F, Tosolini M, Fournie JJ. Single-Cell Signature Explorer for comprehensive visualization of single cell signatures across scRNA-seq datasets. Nucleic Acids Res. 2019;47(21):e133.
40. Gaspar JM. NGmerge: merging paired-end reads via novel empirically-derived models of sequencing errors. BMC Bioinformatics. 2018;19(1):536.
41. Pohl A, Beato M. bwtool: a tool for bigWig files. Bioinformatics. 2014;30(11):1618-9.
42. Schep AN, Wu B, Buenrostro JD, Greenleaf WJ. chromVAR: inferring transcription-factor-associated accessibility from single-cell epigenomic data. Nat Methods. 2017;14(10):975-8.
43. Castro-Mondragon JA, Riudavets-Puig R, Rauluseviciute I, Lemma RB, Turchi L, Blanc-Mathieu R, et al. JASPAR 2022: the 9th release of the open-access database of transcription factor binding profiles. Nucleic Acids Res. 2022;50(D1):D165-D73.
44. Cieri N, Camisa B, Cocchiarella F, Forcato M, Oliveira G, Provasi E, et al. IL-7 and IL-15 instruct the generation of human memory stem T cells from naive precursors. Blood. 2013;121(4):573-84.
45. Boucher JC, Li G, Shrestha B, Zhang Y, Vishwasrao P, Cabral ML, et al. Mutation of the CD28 costimulatory domain confers increased CAR T cell persistence and decreased exhaustion. The Journal of Immunology. 2018;200(1 Supplement):57.28-57.28.
46. Kratchmarov R, Magun AM, Reiner SL. TCF1 expression marks self-renewing human CD8(+) T cells. Blood advances. 2018;2(14):1685-90.
47. Tejera MM, Kim EH, Sullivan JA, Plisch EH, Suresh M. FoxO1 controls effector-to-memory transition and maintenance of functional CD8 T cell memory. Journal of immunology (Baltimore, Md : 1950). 2013;191(1):187-99.
48. Macintyre AN, Finlay D, Preston G, Sinclair LV, Waugh CM, Tamas P, et al. Protein kinase B controls transcriptional programs that direct cytotoxic T cell fate but is dispensable for T cell metabolism. Immunity. 2011;34(2):224-36.
49. Kerdiles YM, Beisner DR, Tinoco R, Dejean AS, Castrillon DH, DePinho RA, et al. Foxo1 links homing and survival of naive T cells by regulating L-selectin, CCR7 and interleukin 7 receptor. Nat Immunol. 2009;10(2):176-84.
50. Chen Z, Arai E, Khan O, Zhang Z, Ngiow SF, He Y, et al. In vivo CD8(+) T cell CRISPR screening reveals control by Fli1 in infection and cancer. Cell. 2021;184(5):1262-80 e22.
51. Cai Q, Medeiros L, Xu X, Young K. MYC-driven aggressive B-cell lymphomas: Biology, Entity, Differential Diagnosis and Clinical Management. Oncotarget. 2015;6.

52. Yang CY, Best JA, Knell J, Yang E, Sheridan AD, Jesionek AK, et al. The transcriptional regulators Id2 and Id3 control the formation of distinct memory CD8+ T cell subsets. Nature Immunology. 2011;12(12):1221-9.
53. Utzschneider DT, Delpoux A, Wieland D, Huang X, Lai C-Y, Hofmann M, et al. Active Maintenance of T Cell Memory in Acute and Chronic Viral Infection Depends on Continuous Expression of FOXO1. Cell Reports. 2018;22(13):3454-67.
54. Klotz LO, Sánchez-Ramos C, Prieto-Arroyo I, Urbánek P, Steinbrenner H, Monsalve M. Redox regulation of FoxO transcription factors. Redox Biol. 2015;6:51-72.
55. Nakae J, Barr V, Accili D. Differential regulation of gene expression by insulin and IGF-1 receptors correlates with phosphorylation of a single amino acid residue in the forkhead transcription factor FKHR. The EMBO journal. 2000;19(5):989-96.
56. Dong E, Yue X-z, Shui L, Liu B-r, Li Q-q, Yang Y, et al. IFN-γ surmounts PD-L1/PD1 inhibition to CAR-T cell therapy by upregulating ICAM-1 on tumor cells. Signal Transduction and Targeted Therapy. 2021;6(1):20.
57. Chmielewski M, Kopecky C, Hombach AA, Abken H. IL-12 Release by Engineered T Cells Expressing Chimeric Antigen Receptors Can Effectively Muster an Antigen-Independent Macrophage Response on Tumor Cells That Have Shut Down Tumor Antigen Expression. Cancer Research. 2011;71(17):5697-706.
58. Larson RC, Kann MC, Bailey SR, Haradhvala NJ, Llopis PM, Bouffard AA, et al. CAR T cell killing requires the IFNγR pathway in solid but not liquid tumours. Nature. 2022;604(7906):563-70.
59. Piechocki MP, Ho YS, Pilon S, Wei WZ. Human ErbB-2 (Her-2) transgenic mice: a model system for testing Her-2 based vaccines. J Immunol. 2003;171(11):5787-94.
60. Wen J, Kawamata Y, Tojo H, Tanaka S, Tachi C. Expression of whey acidic protein (WAP) genes in tissues other than the mammary gland in normal and transgenic mice expressing mWAP/hGH fusion gene. Molecular Reproduction and Development. 1995;41(4):399-406.
61. Mardiana S, John LB, Henderson MA, Slaney CY, von Scheidt B, Giuffrida L, et al. A Multifunctional Role for Adjuvant Anti-4-1BB Therapy in Augmenting Antitumor Response by Chimeric Antigen Receptor T Cells. Cancer Research. 2017;77(6):1296-309.
62. Kantari-Mimoun C, Barrin S, Vimeux L, Haghiri S, Gervais C, Joaquina S, et al. CAR T-cell Entry into Tumor Islets Is a Two-Step Process Dependent on IFNγ and ICAM-1. Cancer Immunology Research. 2021;9(12):1425-38.
63. Kousteni S. FoxO1, the transcriptional chief of staff of energy metabolism. Bone. 2012;50(2):437-43.
64. Monteiro LB, Davanzo GG, de Aguiar CF, Moraes-Vieira PMM. Using flow cytometry for mitochondrial assays. MethodsX. 2020;7:100938.
65. Jang KJ, Mano H, Aoki K, Hayashi T, Muto A, Nambu Y, et al. Mitochondrial function provides instructive signals for activation-induced B-cell fates. Nat Commun. 2015;6:6750.
66. Fraietta JA, Nobles CL, Sammons MA, Lundh S, Carty SA, Reich TJ, et al. Disruption of TET2 promotes the therapeutic efficacy of CD19-targeted T cells. Nature. 2018;558(7709):307-12.
67. Rad SMA, Poudel A, Tan GMY, McLellan AD. Promoter choice: Who should drive the CAR in T cells? PLoS One. 2020;15(7):e0232915.
68. Wherry EJ, Ha SJ, Kaech SM, Haining WN, Sarkar S, Kalia V, et al. Molecular signature of CD8+ T cell exhaustion during chronic viral infection. Immunity. 2007;27(4):670-84.
69. Shan Q, Zhu S, Chen X, Liu J, Yuan S, Li X, et al. Tcf1-CTCF cooperativity shapes genomic architecture to promote CD8(+) T cell homeostasis. Nat Immunol. 2022;23(8):1222-35.

70. Delpoux A, Marcel N, Hess Michelini R, Katayama CD, Allison KA, Glass CK, et al. FOXO1 constrains activation and regulates senescence in CD8 T cells. Cell Rep. 2021;34(4):108674.
71. Lynn RC, Weber EW, Sotillo E, Gennert D, Xu P, Good Z, et al. c-Jun overexpression in CAR T cells induces exhaustion resistance. Nature. 2019;576(7786):293-300.
72. Bansal R, Reshef R. Revving the CAR – Combination strategies to enhance CAR T cell effectiveness. Blood Reviews. 2021;45:100695.
73. Klebanoff CA, Crompton JG, Leonardi AJ, Yamamoto TN, Chandran SS, Eil RL, et al. Inhibition of AKT signaling uncouples T cell differentiation from expansion for receptor-engineered adoptive immunotherapy. JCI Insight. 2017;2(23).
74. Song D-G, Ye Q, Carpenito C, Poussin M, Wang L-P, Ji C, et al. In Vivo Persistence, Tumor Localization, and Antitumor Activity of CAR-Engineered T Cells Is Enhanced by Costimulatory Signaling through CD137 (4-1BB). Cancer Research. 2011;71(13):4617-27.
75. Jadhav RR, Im SJ, Hu B, Hashimoto M, Li P, Lin J-X, et al. Epigenetic signature of PD-1+ TCF1+ CD8 T cells that act as resource cells during chronic viral infection and respond to PD-1 blockade. Proceedings of the National Academy of Sciences. 2019;116(28):14113-8.
76. Utzschneider DT, Gabriel SS, Chisanga D, Gloury R, Gubser PM, Vasanthakumar A, et al. Early precursor T cells establish and propagate T cell exhaustion in chronic infection. Nature Immunology. 2020;21(10):1256-66.
77. Wu T, Ji Y, Moseman EA, Xu HC, Manglani M, Kirby M, et al. The TCF1-Bcl6 axis counteracts type I interferon to repress exhaustion and maintain T cell stemness. Science immunology. 2016;1(6):eaai8593.
78. Utzschneider DT, Charmoy M, Chennupati V, Pousse L, Ferreira DP, Calderon-Copete S, et al. T Cell Factor 1-Expressing Memory-like CD8+ T Cells Sustain the Immune Response to Chronic Viral Infections. Immunity. 2016;45(2):415-27.
79. Rostamian H, Khakpoor-Koosheh M, Fallah-Mehrjardi K, Mirzaei HR, Brown CE. Mitochondria as Playmakers of CAR T-cell Fate and Longevity. Cancer Immunology Research. 2021;9(8):856-61.
80. Huang Q, Wu X, Wang Z, Chen X, Wang L, Lu Y, et al. The primordial differentiation of tumor-specific memory CD8(+) T cells as bona fide responders to PD-1/PD-L1 blockade in draining lymph nodes. Cell. 2022;185(22):4049-66 e25.
81. Reinhard K, Rengstl B, Oehm P, Michel K, Billmeier A, Hayduk N, et al. An RNA vaccine drives expansion and efficacy of claudin-CAR-T cells against solid tumors. Science. 2020;367(6476):446-53.
82. Marchingo JM, Cantrell DA. Protein synthesis, degradation, and energy metabolism in T cell immunity. Cellular & Molecular Immunology. 2022;19(3):303-15.

Figures

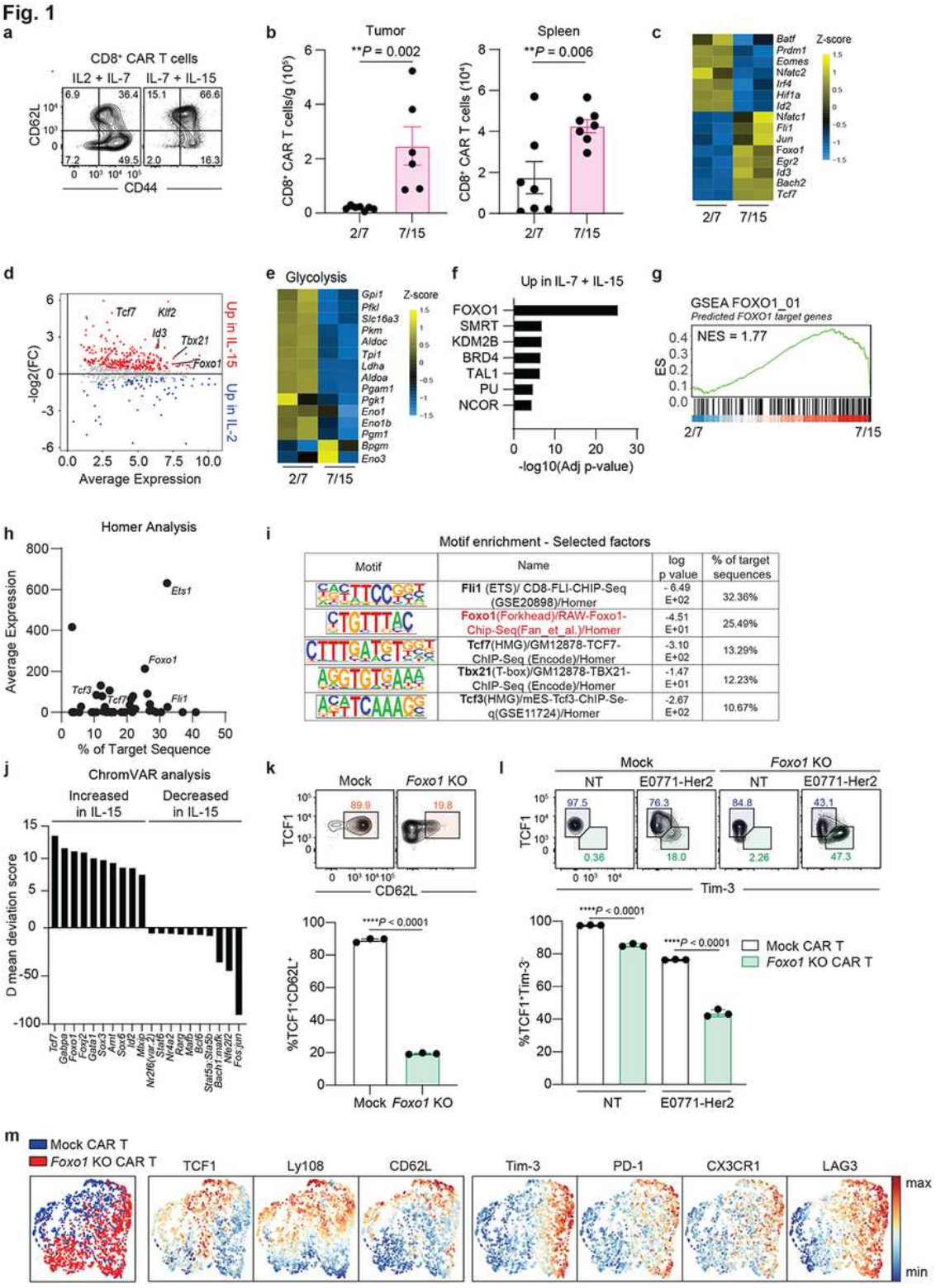

Figure 1

CAR T cells polarized with IL-15 have increased expression of Foxo1

a, Murine anti-Her2 CD8+ CAR T cell expression of CD44 and CD62L following preconditioning with IL-2 and IL-7 or IL-15 and IL-7. b, CAR T cell numbers from tumors and spleens of E0771-Her2 tumor bearing mice at day 9 post treatment following preconditioning with indicated cytokines. c-e, Heatmaps and MA-plot of indicated transcriptional regulators or glycolytic enzymes in CD8+CD62L+ CAR T cells cultured in vitro with indicated cytokines at day 6 post transduction. f-g. Gene set enrichment analyses of CAR T cells from c. relative to the CHEA dataset (f) and in silico predicted FOXO1 target genes (g; FOXO_01; https://www.gsea-msigdb.org/gsea/msigdb/cards/FOXO1_01.html). h-j. CD8+ CAR T cells treated as per c. were analyzed by ATAC-Seq. h-i, Homer analysis of motif enrichment in differentially accessible peaks. The top 50 most significantly enriched motifs in IL-15 conditioned CAR T cells are plotted relative to the percentage of target sequence and average expression in IL-15 cultured CD8+CD62L+ CAR T cells. j, ChromVar analysis of cells from h. Mean deviation score was calculated for the following subsets of CD8+ CAR T cells; cultured in either IL-2 and IL-7 or IL-7 and IL-15; CD62L+CD44+, CD62L+CD44low, CD62L-CD44+. The delta mean deviation score for the CD62L+CD44+ subset cultured in IL-2/IL-7 or IL-7/IL-15 is shown for the top 10 ranking transcription factors in each direction. k-l. anti-Her2 CAR T cells were CRISPR/Cas9-edited to target Foxo1. At day 5 post transduction CD8+ CAR T cells were phenotyped for expression of CD62L and Tcf1 in steady state (k) or serially cocultured with E0771-Her2 tumor cells for 3 consecutive days and expression of indicated markers determined (l-m). a and k-m representative of >3 independent experiments, data points indicate biological triplicates, b, n= 7 mice per group. Bars represent mean ± s.e.m, (**p<0.01). c-j Samples indicative of biological duplicates.

Fig. 2

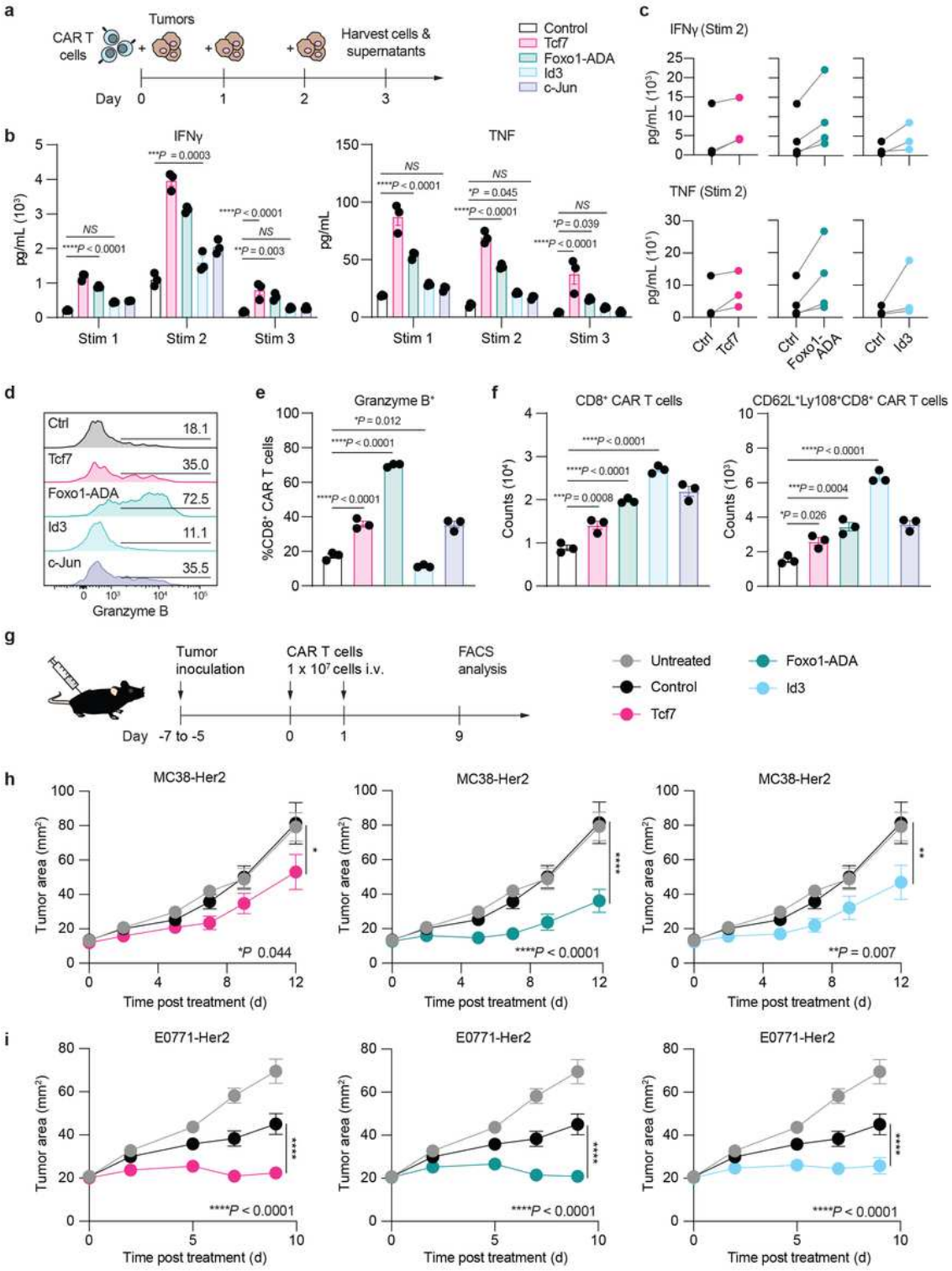

Figure 2

Foxo1-ADA overexpression enhances CAR T cell survival, polyfunctionality 938 and therapeutic activity

a, Schematic of tumor cell coculture assay. b, IFNγ and TNF production following each round of E0771-Her2 tumor cell stimulation with CAR T cells modified via overexpression of indicated transcription factors. c. Paired analyses of n = 4 repeat experiments setup as per b. d-e, Expression of Granzyme B in

CAR T cells following 72 hours of coculture. f, Number of total or CD62L+Ly108+ CD8+ CAR T cells. Bars represent mean ± SD of triplicate samples from a representative experiment of n = 3. Histogram overlays concatenated from biological replicates. g, schematic for in vivo experiments, h-i Treatment of subcutaneous MC38-Her2 or mammary fat pad E0771-Her2 tumors. Tumors were established in mice for 5 to 7 days, prior to treatment with two doses of 1 x 107 indicated CAR T cells administered on subsequent days. b, and e-f one-way ANOVA, representative of at least 3 independent experiments. c, paired Student's T test, (**p <0.01, ***p < 0.001, ****p < 0.0001). h-i, Tumor growth represented as mean tumor size from n = 15-18 mice per group ± SEM from 3 pooled experiments. Two-way ANOVA. (**p <0.01, ****p < 0.0001).

Fig. 3

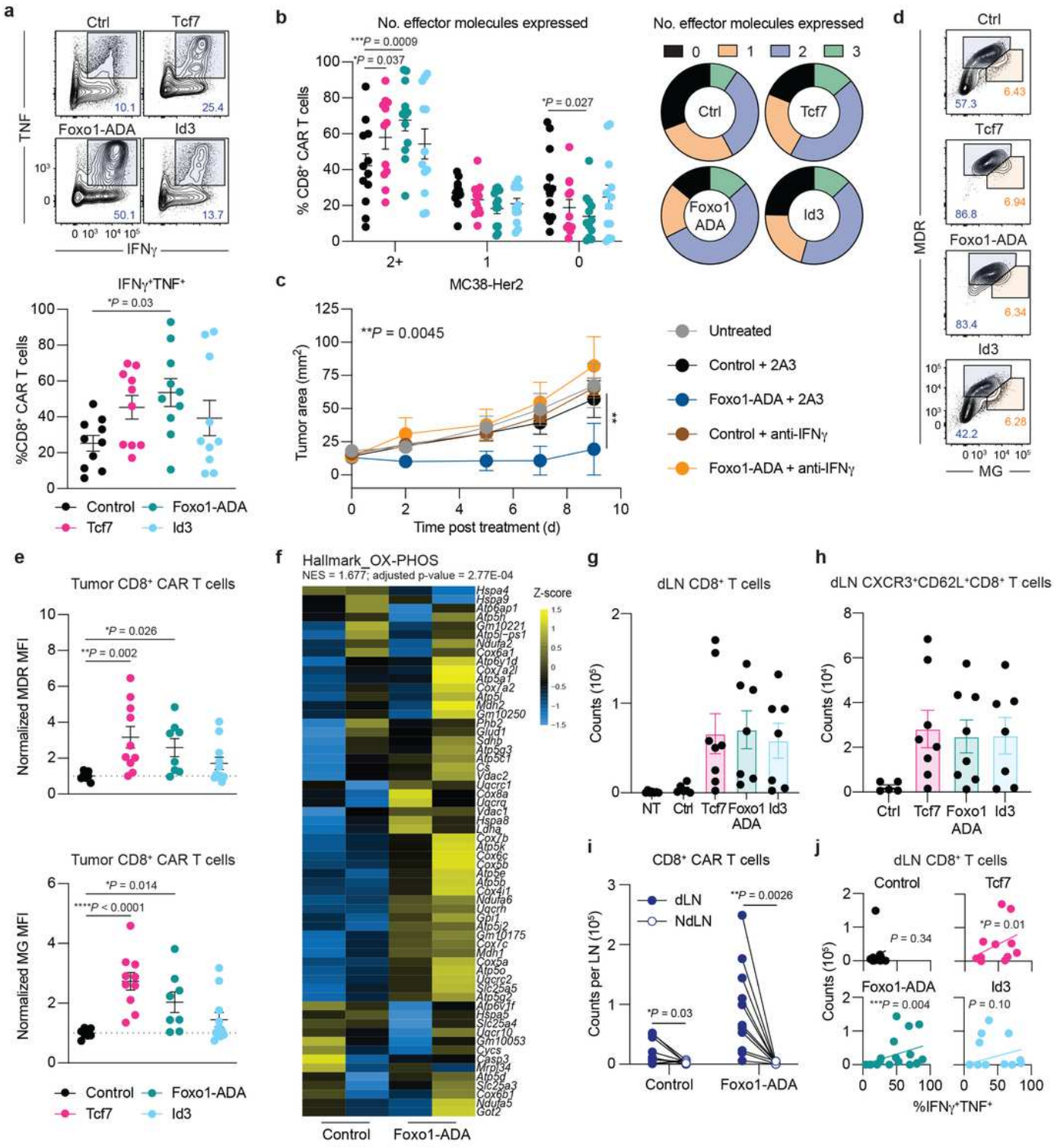

Figure 3

Foxo1-ADA overexpression enhances in vivo polyfunctionality and metabolic fitness

a-d, Flow cytometry analysis of tumor infiltrating CAR T cells from mice bearing E0771-Her2 mammary fat pad tumors at 9-days post treatment. a, Frequency of tumor infiltrating CD8+ CAR T cells expressing IFNγ and TNF. Left panel- concatenated samples from one experiment, right panel- data from individual

mice. b, Frequency of intratumoral CAR T cells expressing 0, 1, 2 or 3 effector proteins of IFNγ, TNF and GzmB. c, MC38-Her2 tumor growth in mice treated as per Figure 2. Where indicated mice were co-treated with anti-IFNγ (H22; 250 μg per mouse) at days -1, 0 and 7 post treatment. d-e, Mitotracker Deep Red (MDR) and Mitotracker Green (MG) staining tumor infiltrating CD8+ CAR T cells. d, staining of concatenated samples e, MDR and MG staining intensity for individual mouse replicates. f, Heatmap for genes in the oxidative phosphorylation Hallmark pathway CD8+ CAR T cells at 72 hours post anti-CAR stimulation. g-j, Flow cytometry analysis of tumor, draining lymph node (dLN) on non-draining lymph node (ndLN) associated CAR T cells from mice bearing E0771-Her2 mammary fat pad tumors at 9-days post treatment. Number of total (g) or CXCR3+CD62L+ (h) tumor dLN resident CD8- CAR T cells. i, Paired analysis of number of CAR T cells in the ndLN and dLN. j, Correlation of number of tumor dLN resident CD8+ CAR T cells to frequency of IFNγ+TNF+ intratumoral CD8+ CAR T cells. a-b, e-i Bars represent mean ± SEM from indicated number of mice pooled from 2 independent experiments, One way ANOVA. c. Data represents the mean ± s.e.m of 3-5 mice per group, Two way ANOVA (*p<0.05, **p <0.01, ****p < 0.0001).

Fig. 4

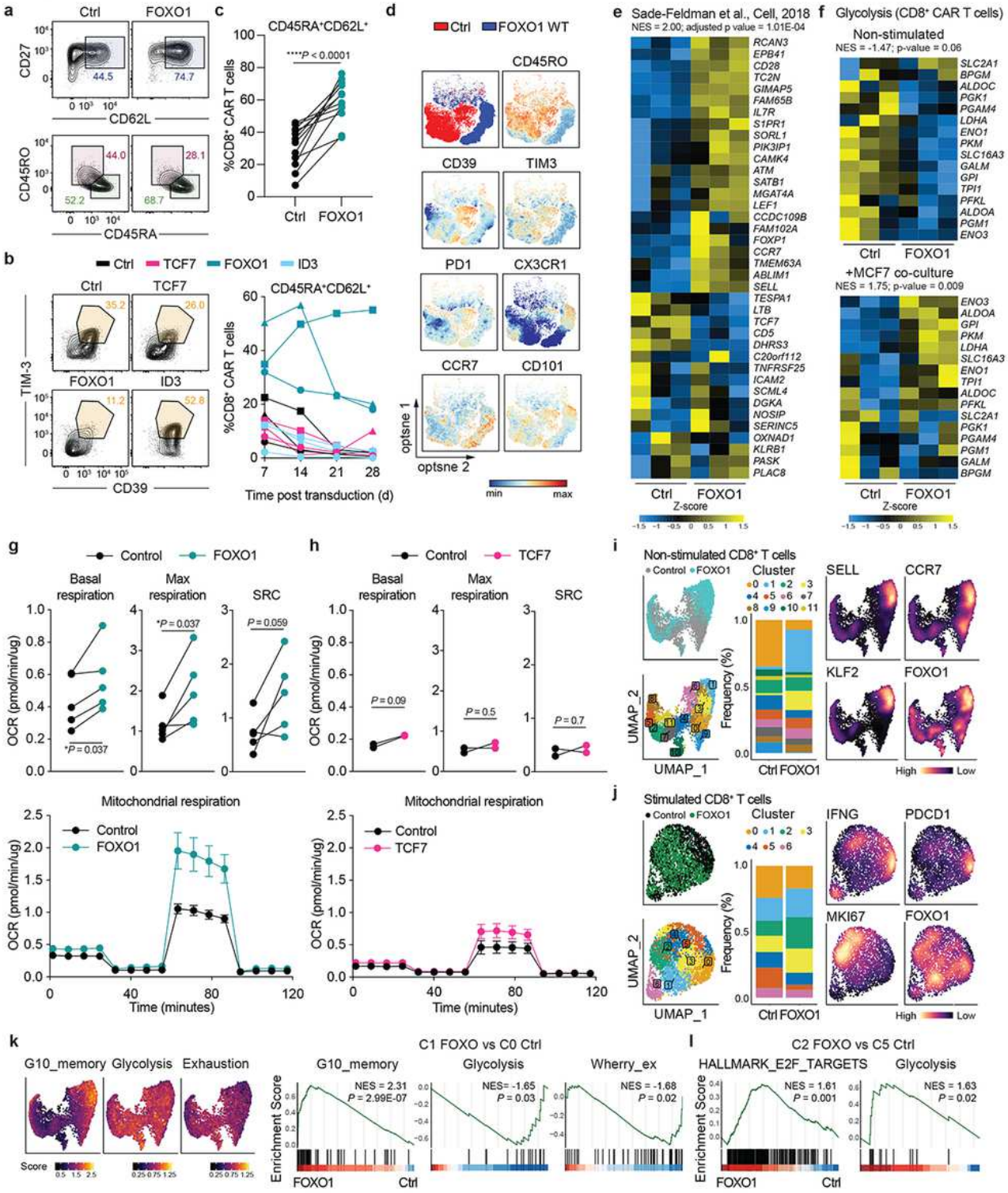

Figure 4

Human CAR T cells overexpressing FOXO1 are resistant to exhaustion and 976 exhibit improved metabolic fitness

Anti-Lewis Y CAR T cells were generated via activation of human peripheral blood mononuclear cells (PBMCs) for 48 hours with IL-2 and OKT3 followed by lentiviral transduction, a-d, The impact of FOXO1,

TCF7 or ID3 overexpression on CAR T cell phenotype was determined a and d, flow cytometry analysis for expression of indicated markers on CD8+CAR+ T cells. b, Left panel as per (a). Right panel indicates the proportion of CD8+ CAR T cells expressing a CD45RA+CD62L+ phenotype. Circles, squares and triangles represent 3 individual donors. Transcription factors are color coded. c. Paired analysis from 12 individual experiments. e-f, CD8+ CAR T cells were analyzed by RNA-Seq before and after activation with MCF7 tumor cells. Data represented by biological triplicates. e, enrichment of genes associated with less differentiated T cells that correlate with improved responses to immune checkpoint blockade in FOXO1 expressing CAR T cells. Heatmap depicts the 38 genes with highest differential expression in the G10 memory cluster identified by Sade-Feldmann et al. f, expression of glycolysis related genes before and after coculture with MCF7 tumor cells. g-h, Analysis of CAR T cell oxidative consumption by Seahorse MitoStress assay following transduction with FOXO1 (g) or TCF7 (h). Data shown represents paired analysis from independent donors (top) or a representative donor (bottom). i-l Control or FOXO1-expressing CAR T cells were left non-stimulated or stimulated for 16 hours with MCF7 tumor cells and then analysed by scRNA-seq. i-j UMAP plots, cell cluster composition and density plots showing expression of indicated genes of of non-stimulated (i) and stimulated (j) CD8+ CAR T cells. k, left- Visualization of gene signatures scores (SingleCellSignature) of memory, glycolysis and exhaustion gene-sets in unstimulated CD8+ T cells right- Gene set enrichment analysis for indicated pathways comparing FOXO1 expressing CAR T cells within cluster 1 to control CAR T cells within cluster 0 (non-stimulated clusters). l, Gene set enrichment analysis for indicated pathways comparing FOXO1 expressing CAR T cells within cluster 2 to control CAR T cells within cluster 5 (stimulated clusters). Statistical significance determined by paired T test (c, g, h). * $p<0.05$, ** $p<0.01$, ***$p<0.001$, **** $p<0.0001$.

Fig. 5

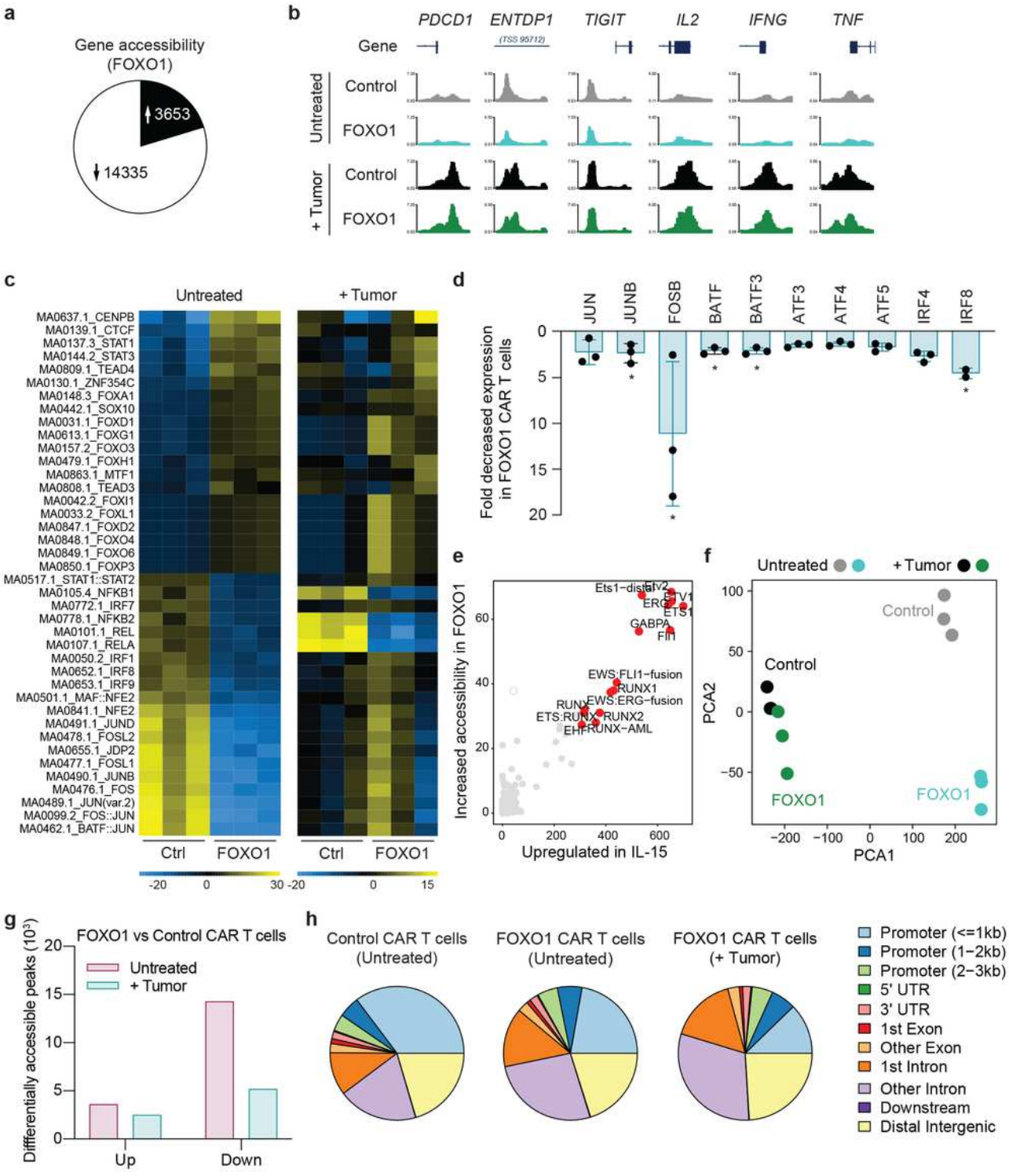

Figure 5

FOXO1 overexpression induces an epigenetic landscape that promotes CAR T cell stemness but does not preclude effector-like transition upon CAR T cell activation.

FOXO1 or control CAR T cells were analyzed by ATACseq 7 days post generation either in the context of no stimulation or after 16 hour coculture with MCF7 tumor cells at a 1:1 ratio. CD8+ CAR T cells were

purified by FACS sorting prior to analysis. Experiment was performed in biological triplicates. a, Differential peak analysis of non-stimulated control or FOXO1-expressing CAR T cells. b, IgV tracks for indicated genes in named CAR T cell groups. c, ChromVAR analysis of motifs (JASPAR) with increased or decreased accessibility in FOXO1-expressing CAR T cells. Heatmap depicts the top 20 motifs in each direction for non-stimulated cells and the same motifs after CAR activation. d, fold reduction in indicated transcription factor expression following FOXO1 overexpression in CD8+ CAR T cells analyzed as per Fig 4e. e, Correlation of motifs with upregulated by IL-15 relative to IL-2 in murine CAR T cells as per Figure 1 and in FOXO1 overexpressing CAR T cells as determined by HOMER analysis. f, PCA of ATAC-seq data for indicated CAR T cell populations. g, Number of peaks with differential accessibility in FOXO1 expressing CAR T cells relative to controls before and after stimulation h, Location of peaks with reduced accessibility in FOXO1-expressing T cells relative to controls prior to stimulation (left) and after MCF7 coculture (right).

Fig. 6

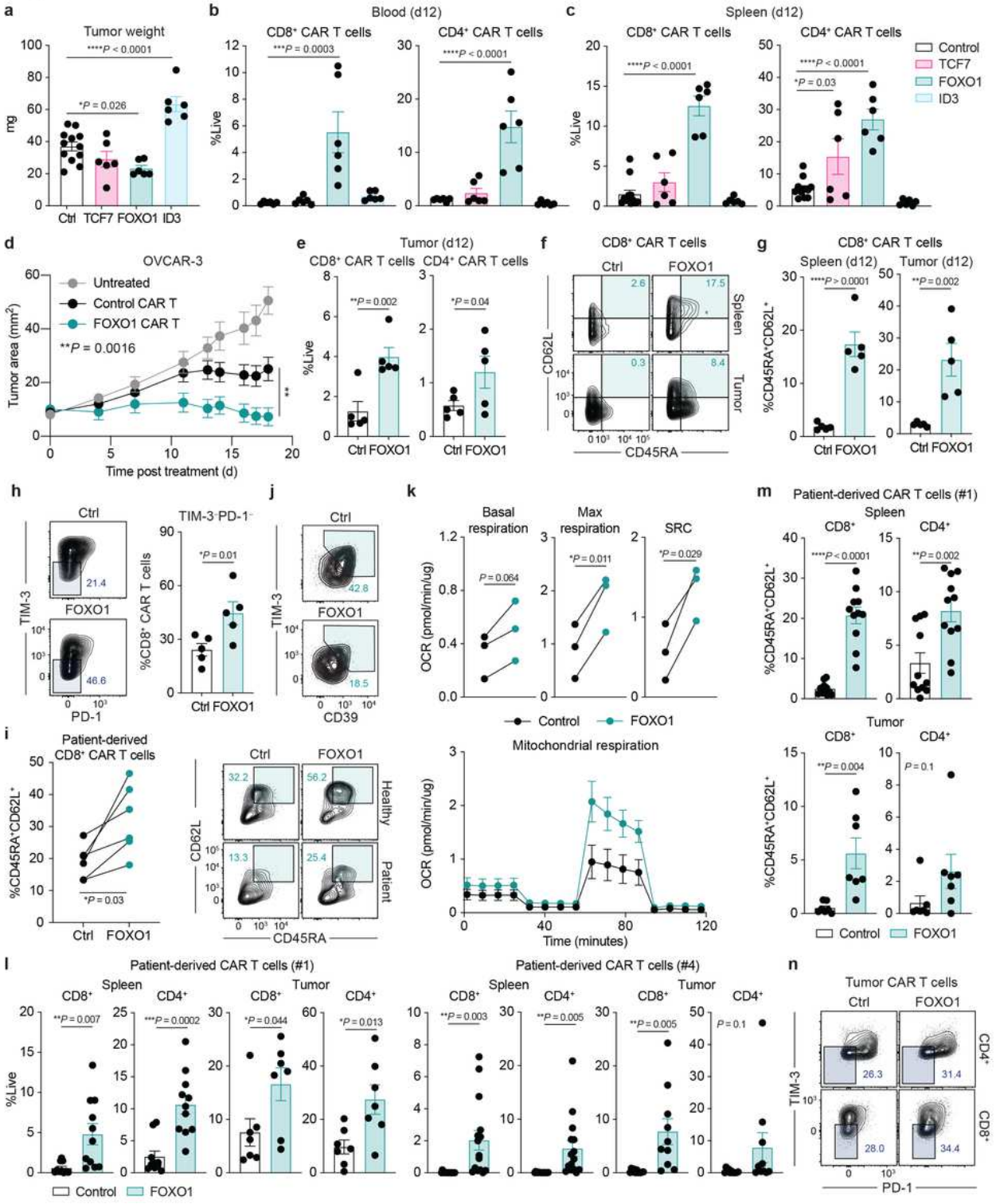

Figure 6

FOXO1 overexpression enhances human CAR T cell efficacy

a. OVCAR-3 tumor weights following 13 days treatment with CAR T cells expressing indicated transcription factor. b-c. Analysis of CAR T cell frequency in the blood (b) and spleens (c) of treated mice at day 12/ 13 post treatment. a-c. Data represents the mean ± SEM of 6 or 12 mice per group. d.

Therapeutic efficacy of anti-Lewis Y CAR T cells utilized to treat mice bearing OVCAR-3 tumors. Data represents the mean ± SEM of 7 mice per group from a representative experiment of n = 2. e-h. Analysis of CAR T cell frequency and phenotype in the spleens and tumors of treated mice at day 12 post treatment. Data represents the mean ± SEM of 5 mice per group. i, Proportion of CD8+ T cells exhibiting a CD45RA+CD62L+ phenotype in CD8+ CAR T cells generated from six patients enrolled onto a CAR T cell trial. J, Expression of TIM3 and CD39 on CD8+ CAR T cells derived from patients. k. Analysis of patient-derived CAR T cell oxidative consumption by Seahorse MitoStress assay following transduction with FOXO1 k. Data shown represents paired analysis from independent donors (left) or a representative patient (right). l-m Analysis of CAR T cell frequency (l) and phenotype (m) in the spleens and tumors of mice treated with patient derived CAR T cells at day 13 post treatment. Data represents the mean ± SEM of 7-15 mice per group. Statistical significance determined by one way ANOVA (a-c), two way ANOVA (d), unpaired t test (e, g, h, l, m) or paired T test (i, k) * $p<0.05$.

Supplementary Files

This is a list of supplementary files associated with this preprint. Click to download.

- SuppFigure105092023.ai
- SuppFigure205092023.ai
- SuppFigure305092023.ai
- SuppFigure405092023.ai
- SuppFigure505092023.ai
- SupplementaryFigure605092023.ai
- SuppFigure705092023.ai
- SuppFigure805092023.ai
- SuppFigure905092023.ai
- SuppFIgure1007092023CS28copy.ai